# Final Report

May 2025

## Student Project No. CTP_FCR_2020_11

### Title: Understanding resistance to *Botrytis cinerea* in strawberries

Finlay Bourquin (1,3), Helen Cockerton (2), Jordan Price (1), Matthew Dickinson (3), Tim Robbins (3), Charlotte Nellist (1)

*(1) National Institute of Agricultural Biology, UK*
*(2) University of Kent, UK*
*(3) University of Nottingham, UK*

**Report No:** [AHDB Use only]

This is the final report of a PhD project that ran from October 2020 to May 2025. The work was funded by BBSRC

# CONTENTS

# 1. Industry Summary

The necrotrophic pathogen *Botrytis cinerea* is pervasive on UK strawberry farms and is one of the most commonly reported strawberry fungal pathogens (Calleja, 2011). UK strawberry production has increased from 35,000 tonnes in 1960 to 119,000 tonnes in 2022 (FAOSTAT, 2022), and as of yet there are no resistant strawberry varieties to *B. cinerea* (Bestfleisch *et al*., 2014; González *et al*., 2009). Currently, the most effective control methods are fungicides, however, *B. cinerea* can recurrently develop resistance to multiple fungicides (Kretschmer *et al*., 2009; Leroch *et al*., 2011). Moreover, there are negative public opinions regarding fungicide residues on food and in the environment, calling for alternative control methods to be adopted (Sutton, 1990).

This project aimed to improve our understanding of how *B. cinerea* causes disease and how strawberries can resist it. The project consisted of two main objectives:

- Identifying strawberry genes linked to resistance by infecting a mutant population of strawberry plants and sequencing those that showed more or less disease than normal.
- Discovering *B. cinerea* virulence genes by comparing the genomes of fungal isolates that varied in how aggressive they were.

Key outcomes:

- New assays were developed to measure infection on strawberry leaves, fruit, and flowers, enabling robust testing of both fungal isolates and mutant strawberry plants.
- A total of 774 strawberry genes of interest were identified, with 13 showing potential links to disease resistance.
- *B. cinerea* isolates were ranked by aggressiveness, and genes unique to the most aggressive isolates were identified.

Why this matters:

- The strawberry resistance genes discovered could help breeders develop more resistant strawberry varieties, reducing the need for fungicides.
- The fungal genes identified may act as targets for environmentally friendly control tools, such as RNA interference (RNAi) sprays.
- Farmers could benefit from reduced pre-harvest losses, while retailers and consumers would see longer shelf-life post-harvest.

This work lays the foundation for more sustainable, effective control strategies against *B. cinerea* whilst improving strawberry resistance, in order to aid the UK strawberry industry to increase yields.

## 2. Introduction

Strawberry production is not only increasing globally, from 754,516 tonnes in 1961 to 9,569,865 tonnes in 2022, but it is also increasing in the UK, from 35,000 tonnes in 1960 to 119,000 tonnes in 2022 (FAOSTAT, 2022). Increasing strawberry production is important since the world population is increasing (World Population Prospects, 2024) and strawberries have many benefits for human health, such as, reducing the risks of diabetes, cardiovascular diseases, cancer and anaemia (da Silva Pinto *et al*., 2010; Kurniati *et al*., 2021; Zhang *et al*., 2008). Moreover, strawberries are beneficial for weight management due to their low glycaemic load (Dreher & Ford, 2020), which is particularly important considering the rise in obesity levels, from 8.7 million in 2000 to 14.3 million in 2022 in the UK (FAOSTAT, 2022). Currently, strawberries require the most land per kilogram to produce, among fruit assessed in Clark *et al*. (2022). Therefore, to meet increasing food demands by a growing population and limiting land-use, improving strawberry production efficiency is essential.

Furthermore, climate change, through increasing drought, temperatures and altered humidity levels, is expected to negatively impact crop yields and increase crop susceptibility to fungal pathogens (Sewelam *et al*., 2021; Trenberth, 2011). *Botrytis cinerea*, the causal agent of grey mould, is the most reported strawberry pathogen on UK farms (Calleja, 2011) and in the absence of fungicides and high humidity *B. cinerea* has been reported to cause over 80% of fruit and flower losses (Ries, 1995). Conventional management strategies such as weeding, increasing air circulation and ensuring proper soil drainage are insufficient alone (Daugaard, 1999). Fungicides are the most effective control method, however, *B. cinerea* can become resistant to multiple fungicides (Kretschmer *et al*., 2009; Leroch *et al*., 2011) and there is an increasing negative public perception of fungicide residues on food (Sutton, 1990). Therefore, alternative control methods need to be investigated. Through examining the molecular mechanisms of the strawberry-*B. cinerea* interactions, candidate plant disease resistance factors and fungal virulence factors can be identified and facilitate the development of new control methods to mitigate crop losses.

In order to discover novel disease resistance factors and fungal virulence factors the following objectives were investigated:

1) Investigate *B. cinerea* aggressiveness across hosts and across host organs.

Pathogenicity assays were developed for all strawberry host organs in order to obtain a quantitative measure of aggressiveness for ten *B. cinerea* isolates.

2) Identify novel resistance factors to *B. cinerea* in ethyl methanesulfonate (EMS) mutated *Fragaria vesca* plants

The most virulent isolate, deduced from objective 1, was used to infect mutant *F. vesca* plants. Plants with altered susceptibility underwent DNA extraction, genome sequencing and bioinformatics were conducted to identify the genes that could be responsible.

3) Identify novel *B. cinerea* virulence factors across hosts and within host organs

Bioinformatics was carried out to identify secreted effectors that were associated with the isolate aggressiveness rankings from objective 1.

# 3. Materials and methods

## 3.1. Developing pathogenicity assays

### 3.1.1. Leaf pathogenicity assay

Emerging unfolded trifoliate *F. vesca* leaves were marked with tape around the petioles. At two-weeks-old leaves were surface sterilised in 0.5% sodium hypochlorite for 3 min, washed in 70% ethanol, washed in sterile distilled water (SDW) twice and dried in a laminar flow hood. Leaf discs were cut using a 1 cm diameter cork borer, wounded at the centre using a sterile 16 G needle and placed onto 1.5% WA in 5 x 5 compartmentalised Petri dishes (Figure 1). Spores were harvested from ten 3-week-old *B. cinerea* isolates (Table 1), cultured on PDA, by dislodging them with 5 mL SDW, filtered through Mira cloth to remove mycelia, and adjusted using a haemocytometer to spore concentrations of 5 x $10^5$ / mL. A volume of 10 µL of spore suspension, or SDW for the control, was inoculated onto the leaf disc wound. The inoculated leaves were incubated at 25 ˚C with a 16 h day / 8 h night cycle. This experiment was repeated four times for a total of 451 leaf discs. Inoculum from isolates were randomised using the R (R Core Team, 2020) package ‘blocksdesign’ (Edmondson, 2021). Every 24 h for 18 days an image was taken with a digital single-lens reflex (DSLR) camera, using a light box and light panels to maintain consistent lighting. The images were analysed using ImageJ (Abràmoff *et al*., 2004) to measure lesion size per leaf disc. The colour threshold hue was set to 0-30 to isolate brown pixels. The image was then converted to black and white, to represent disease and healthy tissue respectively, and the ratio of black to white pixels was taken as a measure of leaf disc disease.

**Table 1.** *Botrytis cinerea* isolates investigated in this study.

| Isolate | Host plant isolated from | Date isolated | Source |
|---|---|---|---|
| R36/19 | Cox apple | 11.04.2019 | Mansfields (FWM) Chartham coldstore |
| R4/20 | Strawberry | 27.08.2020 | Ditton Rough, East Malling Research |
| CHF | Strawberry | n/a | n/a |
| B104 | n/a | 18.05.1994 | n/a |
| 21010 | Apple | 24.07.1998 | n/a |
| 21018 | Raspberry cane | 25.11.2005 | East Malling Research |
| 21019 | Raspberry fruit | 25.11.2005 | East Malling Research |
| 21024 | Tomato | 10.02.2006 | n/a |
| Bc19 | Tomato | n/a | n/a |
| Nos6 | Rose | n/a | n/a |

**n/a = not available**

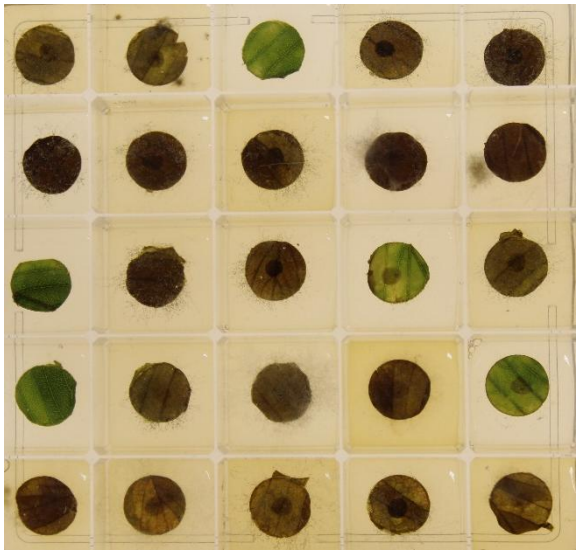

**Figure 1.** Example set-up of the pathogenicity experiment on *Fragaria vesca* leaves. Leaves were cut to 1 cm in diameter and placed in 5 x 5 Petri dishes prior to being inoculated with 10 µL of *B. cinerea* spore suspensions (5 x $10^5$ / mL).

### 3.1.2. Fruit pathogenicity assay

The calyx were cut off ripe *F.* × *ananassa* cv. Malling Centenary fruits, the fruits were surface sterilised in 0.5% sodium hypochlorite, washed twice with SDW and dried in a laminar flow

hood. The fruit were cut in half and both halves were wounded half a centimetre deep with a 16 G needle, in the centre of the outer surface. One half was inoculated with 10 µL of 5 x $10^5$ / mL spore suspension and the other half inoculated with 10 µL SDW as a control. The strawberries were placed on sterilised filter paper in a 46 × 15 cm metal tray with 4.5 x 4.5 cm individual compartments for each half of the berry (Figure 2). Isolates 21024, 21010, CHF and Bc19 were used and the treatment of spore suspension was randomised using the R (R Core Team, 2020) package 'blocksdesign' (Edmondson, 2021). The tray of inoculated fruit was placed in a clear autoclave bag to maintain humidity and incubated at 10 ˚C with a 16 h day / 8 h night cycle. The height and diameter of each fruit was measured with calipers prior to inoculation. For ten days, the height and width of lesions were measured using calipers, and the average of these two measurements was used to produce a representative diameter of the lesion. The averaged diameter of the lesion was then divided by the averaged diameter of the fruit to obtain the disease incidence per day, with fruits being standardised to have a maximum 1 cm difference in diameter to limit fruit size confounding lesion size. Fruits were measured for ten days, and the experiment was repeated three times to give a total of 80 fruits.

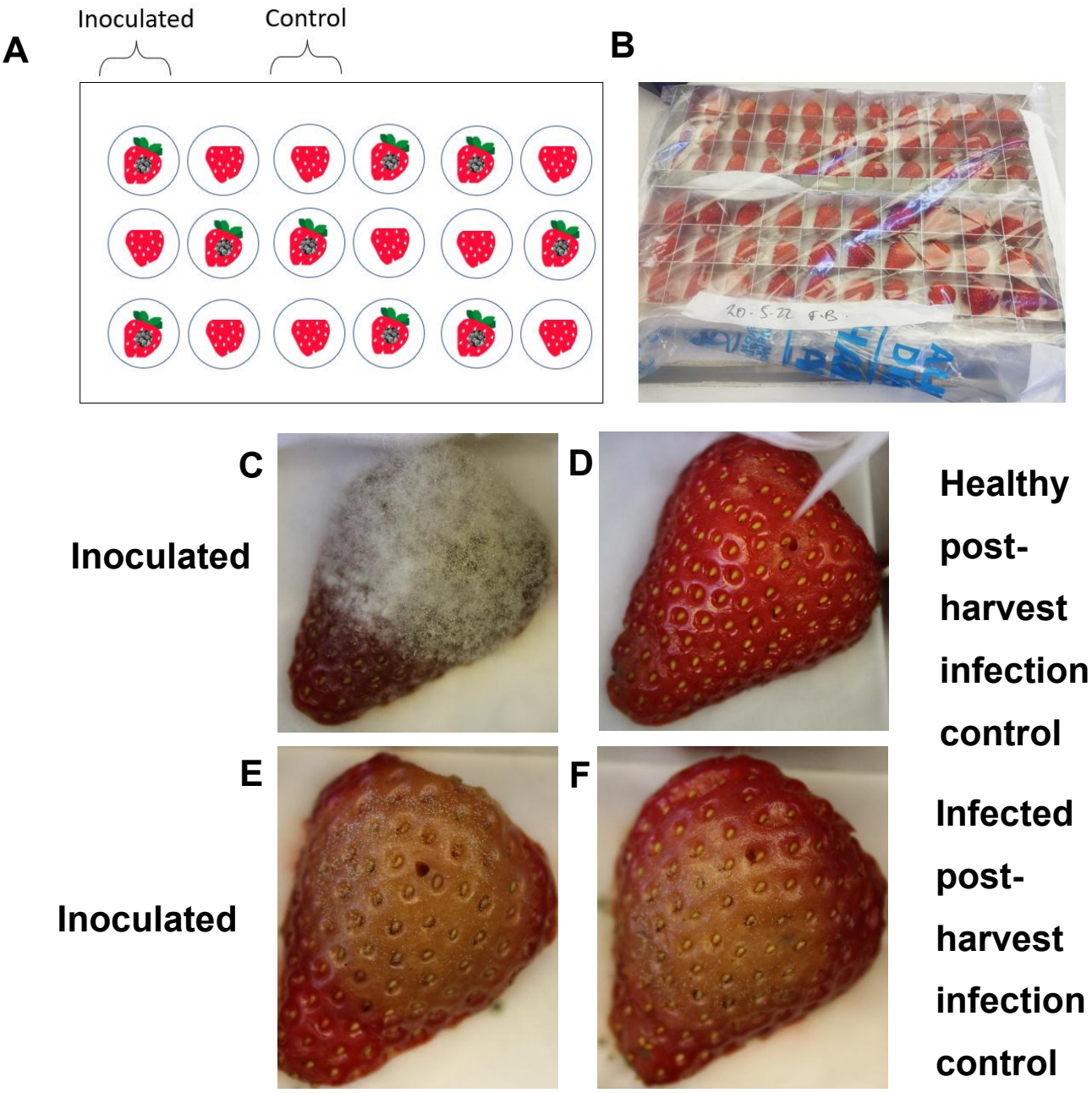


**Figure 2.** Example set-up of the pathogenicity experiment on *Fragaria* × *ananassa* fruit. Sepals were removed and fruits were surface sterilised, cut in half and wounded. One half was inoculated with 10 µL of 5 x $10^5$ / mL *Botrytis cinerea* spore suspension and the other with SDW as a control, prior to incubation for ten days during which lesions were measured daily. **A)** Example layout of the two fruit halves. **B)** Photograph showing the set-up of the pathogenicity experiment. **C-F)** Example of two inoculated fruits with their respective control fruits, one healthy and one exhibiting symptoms of post-harvest infection.

### 3.1.3. Flower pathogenicity assay

Isolates 21024, 21010 and Bc19 were chosen for the stamen pathogenicity experiment. Flowers were placed into 1.5% water agar (WA) at the closed bud stage at 25 ˚C with a 16 h day / 8 h night cycle for 48 h till they reached anthesis. The petals were removed and 20 µL of one-day-old spore suspensions at a concentration of 5 x $10^5$ / mL, or SDW for the control, were transferred onto the stamens with a paintbrush (Figure 3). The flowers were then incubated at 25 ˚C with a 16 h day / 8 h night cycle for four days and the experiment was conducted three times. The stamens were removed from the flower with sharp curved end tweezers and images were taken using a LEICA DFC295 microscope. The images were analysed using ImageJ (Abràmoff *et al*., 2004); a total of 118 stamens were traced freehand, avoiding the anthers, and the mean pixel intensity was measured.

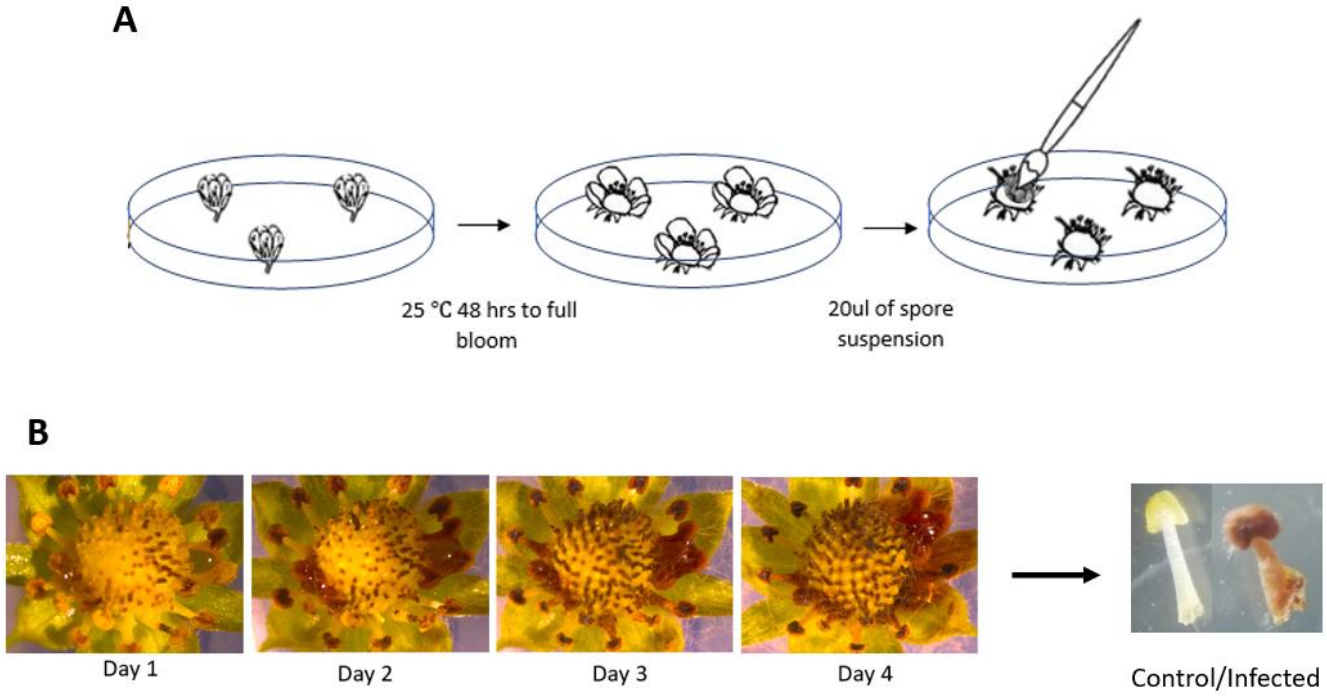


**Figure 3.** An example of the set-up for a *Fragaria vesca* flower pathogenicity assay utilising *Botrytis cinerea.* **A)** Flower buds were placed in water agar and once opened they were inoculated with 20 µL of 5 x $10^5$ / mL spore suspension. **B)** The flowers were incubated for four days, and the stamens were cut off for image analysis, where the mean pixel intensity was used as a measure of disease.

### 3.1.4. Statistical analysis for pathogenicity experiments

The area under the disease progression curve (AUDPC) for the leaf and fruit assays were calculated using the R package 'agricolae' (Mendiburu & Yaseen, 2020). A Kruskal-Wallis rank sum test (Kruskal & Wallis, 1952) was performed to examine the effect of isolates on the AUDPC for leaf and fruit assays and the effect isolates had on the mean pixel intensity for the flower assay. Post-hoc pairwise comparisons were conducted using a Dunn Test, with the Benjamini-Hochberg method to account for multiple comparisons. Spearman's rank correlation analysis was carried out to evaluate the relationship between isolate virulence on *F. vesca* leaves and growth rate. The standard deviation (SD) for the AUDPC values was calculated for each isolate per experiment using the R package 'dplyr' v1.1.4. (Wickham *et al*., 2023).

## 3.2. Identifying novel strawberry resistance factors

### 3.2.1. EMS mutagenesis of *Fragaria vesca* achenes

*F. vesca* accession 'Hawaii 4' achenes were imbibed in 0.01% Tween 20 for 15 min and washed until all residue was removed. Achenes were then soaked in SDW at 4 ºC on a cell mixer overnight. Achenes were treated with an EMS concentration of 0.4% in a fume hood; EMS, or SDW for the control, was injected under the surface of SDW. Falcon tubes were placed on a shaker for 5 min until the oily droplets of EMS had dispersed. Approximately 1,200 achenes were placed in 7 x 10 cm cloth bags per treatment prior to being submerged into 30 mL of EMS solution and incubated for 4 and 8 h.

Following incubation of achenes, the EMS solution was decontaminated by pouring into 10 M NaOH. The achene bags were rinsed with 30 mL of water six times, soaked in 50 mL water for 15 min then placed into a beaker of SDW on a rotary shaker at room temperature. The SDW was changed a further six times over the period of an hour. The achenes from treatment three and four were sown onto Levington Advance® M2 compost one day post treatment in 12 x 8 cell seed trays. Plants were maintained in a glasshouse, set at 23 ºC during the day and 18 ºC at night with a 16 h day / 8 h night cycle. After five weeks the plants were repotted into 11 x 11 cm pots with a nursery mix composed of 20% 8-16 mm composted bark, 40% peat 0-8 mm, 40% peat 8-16 mm, Osmocote Exact Standard 5/6 m 15-9-12+2MgO+TE– 3 g/L incorporated, Start&Gro 0.8 g/kg incorporated and H2Grow wetter granules 0.5 g/kg incorporated. Post germination, chlorotic sectoring was recorded weekly in *F. vesca* seedlings for two months. Fungicides TAKUMI SC® (active ingredient: cyflufenamid, 100 g/L) and Karma SP® (active ingredient: potassium hydrogen carbonate, 850 g/kg) were applied as per the manufacturer's instructions, to control for powdery mildew infection, moreover, biocontrols

Californiline® (predatory mite: *Amblyseius californicus*, Bioline AgroSciences Ltd.) and *Aphidius colemani* were applied to control spider mite and aphid populations respectively.

### 3.2.2. Generating an $M_2$ population

After three months 1,000 $M_1$ plants were self-fertilised to generate an $M_2$ population for *B. cinerea* pathogenicity screening. To self-pollinate individual *F. vesca* plants, wooden sticks were placed in the corners of the strawberry pots and the plants were wrapped in horticultural fleece tied with Velcro ties, to prevent cross-pollination from other individuals (Figure 4). During anthesis, flowers were hand-pollinated using 3 cm soft-bristled lip brushes, one per plant, pollen was transferred through brushing the anthers and subsequently the stigmas. Hand-pollination was carried out two or three times per flower either daily or every other day. Fruits started to ripen around four weeks after pollination and were continuously collected in month four and five after sowing. Once fruit reached the mature ripe stage, they were collected and placed in an incubator at 25 ºC until dried, allowing achenes to be scraped from the fruit. The collected $M_2$ achenes were surface sterilised in 0.5% sodium hypochlorite for 10 min followed by soaking in SDW for 5 min four times. In month six the sterilised achenes were sown onto Levington Advance® M2 compost in a glasshouse at 18 ºC during the day, 15 ºC at night and a 16 h day / 8 h night cycle. A total of 20 achenes were sown per $M_1$ plant. After six weeks, four seedlings from each line were repotted and grown under the aforementioned conditions, providing four daughter $M_2$ plants per $M_1$ plant. The $M_2$ mutants were named based on the EMS treatment: '3' for 0.4% EMS with a 4-hour incubation, or '4' for 0.4% EMS with an 8-hour incubation, the $M_1$ plant from which the achene originated and the specific daughter plant ID e.g. ‘3-70-4’. Visual mutations in the size, colour, and shape of leaves, fruits, and flowers were recorded weekly for 11 weeks.

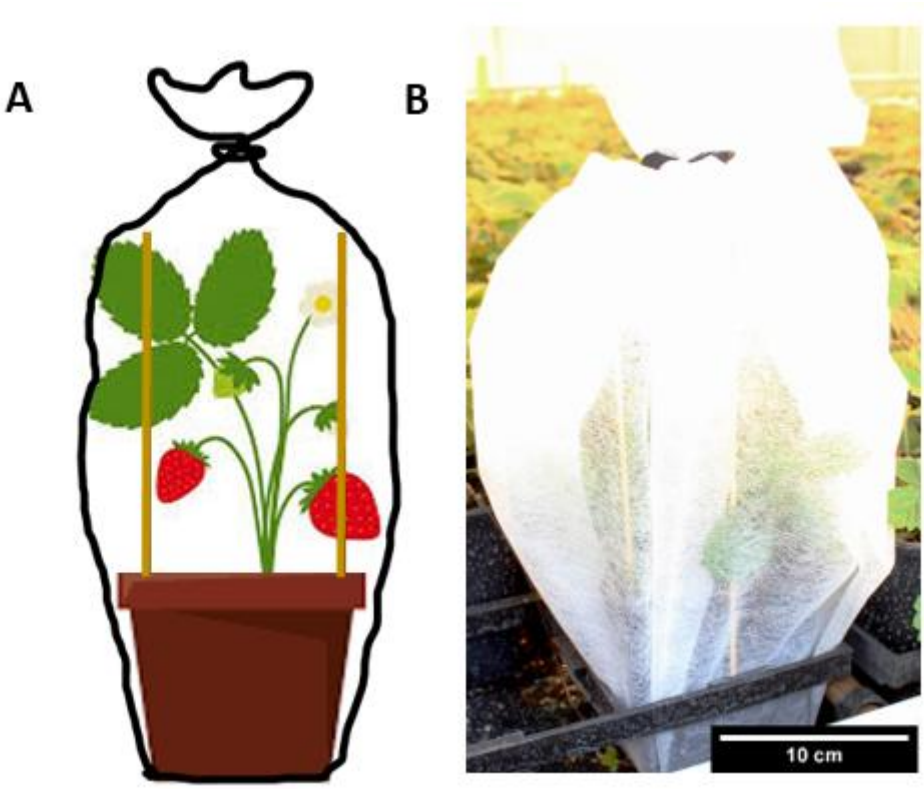


**Figure 4.** Example of *Fragaria vesca* plant set-up to facilitate self-pollination. **A)** Cartoon demonstrating wooden sticks placed in each corner of the pots and the whole plant being wrapped in horticultural fleece. Created with Biorender.com. **B)** Photo of *F. vesca* plant set-up for self-pollination.

### 3.2.3. Pathogenicity experiments

The *B. cinerea* isolate 21024 was selected for use in pathogenicity assays, as it was previously shown to be the most aggressive isolate on *F. vesca* leaves (see **Section 4.1.1**). The pathogenicity experiments were conducted as outlined in **Section 3.1.1**.

### 3.2.4. Experimental design

A total of 270 $M_2$ mutants and ten wild type (WT) control $F_2$ plants were chosen for pathogenicity testing. The $M_2$ mutants were chosen if they appeared healthy, had leaves large enough to collect leaf discs from and they exhibited any visual mutations. The experiment in **Section 3.3.3.** was repeated three times with five leaf discs, four inoculated and one SDW control, per plant and per experiment. Due to technical limitations in collecting, sterilising, cutting, preparing spore suspensions, and inoculating leaf discs from more than 100 plants at a time, each experiment was conducted in batches of 100 plants, resulting in a total of nine

batches (Figure 5). Each batch consisted of 90 mutant plants and ten WT plants. A total of 4,050 leaf discs were assessed, with images taken daily resulting in 56,700 individual leaf disc images. A randomized split block design was used to assign plants to batches, plates to shelves in the incubator and leaf discs within Petri dishes. The designs were generated in R (R Core Team, 2020) using the package ‘blocksdesign’ (Edmondson, 2021). Throughout the experiment plants were pruned to control pest and disease pressure every two weeks.

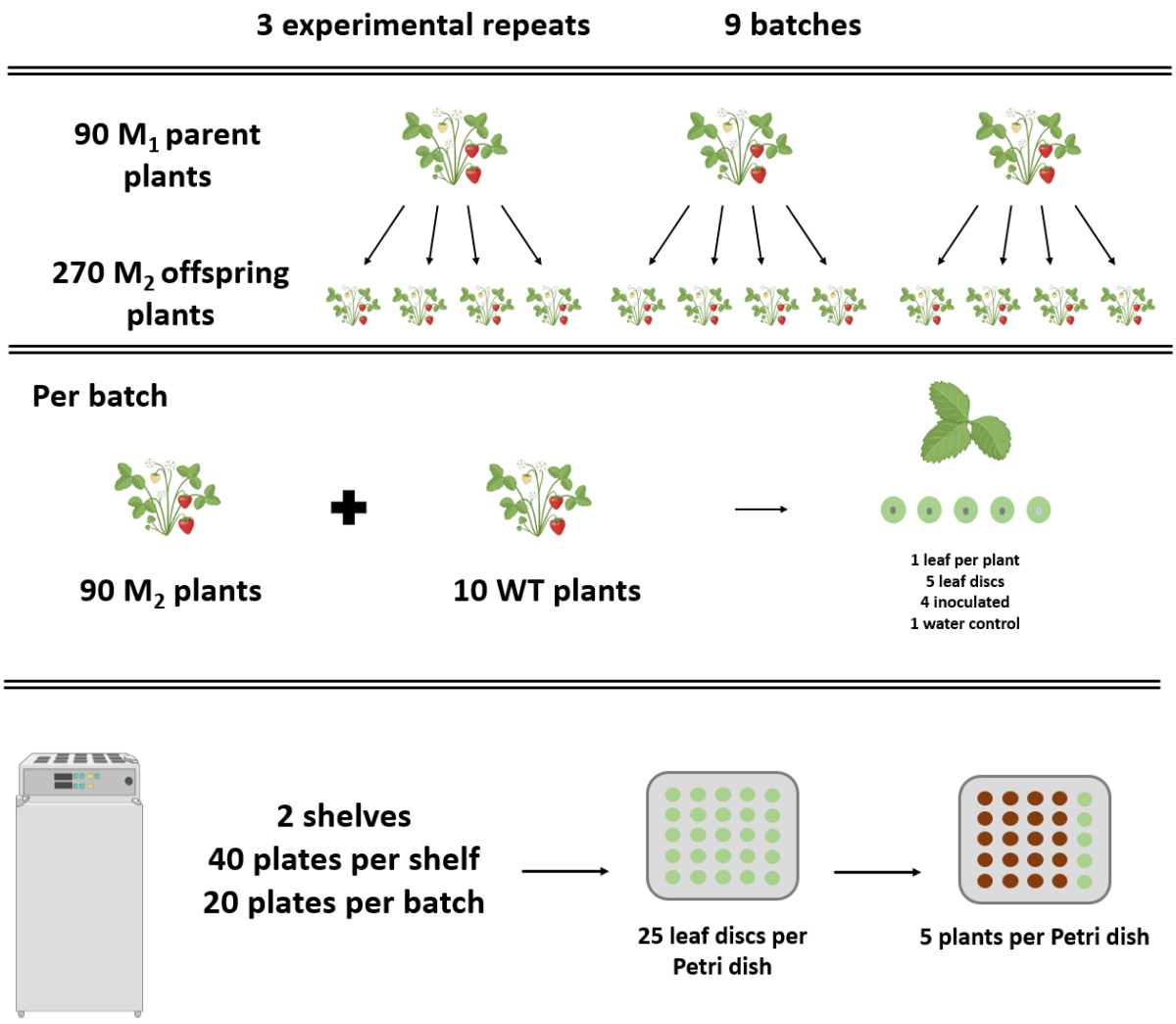


**Figure 5.** Example of the experimental set-up for carrying out pathogenicity assays on 270 ethyl methanesulfonate (EMS) treated *Fragaria vesca* 'Hawaii 4' plants. The experiment was split into three batches per experimental repeat, with three experimental repeats in total. From 90 $M_1$ parent plants, four offspring plants were chosen per parent resulting in 270 $M_2$ plants. Each batch consisted of 90 $M_2$ plants and ten wild type (WT) plants. For every plant, five leaf discs from one two-week-old leaf were inoculated with either a *Botrytis cinerea*, isolate 21024, spore suspension of 5 x $10^5$ / mL or water. Leaf discs were placed in a 5 x 5 compartmentalised Petri dish, allowing for 25 leaf discs which equates to five $M_2$ plants per Petri dish. A total of 40 Petri dishes were produced per experiment and distributed across two shelves

### 3.2.5. Image analysis

Image analysis was conducted using the software 'dishy' (Tang, 2022), written for this project to individually analyse leaf discs on a 5 x 5 compartmentalised Petri dish and subsequently quantify the ratio of brown to green pixels per leaf disc (https://githuB.com/jeremyt0/dishy).

### 3.2.6. Statistical analyses

Mutants that did not provide enough leaf material across all replicates were removed from the dataset. The final data set comprised of 202 mutant plants. To investigate whether or not mutant plants were more or less susceptible than the WT, dose-response curve (DRC) analyses were conducted utilising the package '*drc'* (Ritz & Streibig, 2005). A three-parameter log-logistic model was the most appropriate after comparing various log-logistic and Weibull models using the function 'mselect'. The three-parameter log-logistic model was calculated with the following equation, where *y* was the response at dose *x, d* was the upper asymptote, *e* was the effective dose ($ED_{50}$) and *b* was the slope:

$$y = \frac{d}{1+\left(\frac{x}{e}\right)^{b}} \quad (2)$$

The 'EDcomp' function was used to compare mutant and WT disease progression at time points $T_{30}$, $T_{50}$, $T_{70}$ and $T_{90}$. *P*-values were adjusted using the Benjamini-Hochberg method.

### 3.2.7. DNA extractions

DNA was extracted from mutants that exhibited a statistically significant difference in disease progression from the WT. Prior to DNA extractions, unfolded trifoliate leaves were covered with tinfoil, for one to two days, to limit chlorophyll production. DNA extractions were carried out using the DNeasy® Plant Mini Kit (QIAGEN) following the manufacturer's protocol. Briefly, 100 mg wet weight of plant tissue was ground in liquid nitrogen with a mortar and pestle, lysed in Buffer AP1 and RNase A, incubated at 65 °C for 21 min and inverted every 7 min. The lysate was mixed with Buffer P3 and incubated on ice, followed by centrifugation for 5 min at 20,000 x *g*. The supernatant was transferred to a QIAshredder spin column, centrifuged for 2 min at 20,000 x *g* and the flow-through was combined with Buffer AW1. The mixture was transferred to a DNeasy Mini spin column, washed with Buffer AW2, and the DNA was eluted in 50 µL Buffer AE. DNA quality was assessed with a NanoDrop™ OneC Microvolume UV-Vis Spectrophotometer and the concentration was verified on an Invitrogen™ Qubit™ 3 Fluorometer. Samples were sent for sequencing if the OD260/280 = 1.8-2.0, the OD260/230 ≥ 2 and they had a concentration of ≥ 10 ng/µL.

### 3.2.8. Sequencing

Upon submission to Novogene, the extracted DNA underwent quality control, library preparation, and were sequenced on the Illumina NovaSeq 6000 platform with a paired-end read length of 150 bp.

### 3.2.9. Variant calling

Variant calling was carried out following the pipeline summarised in Figure 6. Quality control checks on the raw sequencing data were performed using FastQC v0.12.0 (Andrews, 2010), both before and after trimming and adapter removal with Trimmomatic v0.39 (Bolger *et al*., 2014). Trimmed reads were mapped to the reference *F. vesca* genome v4.0.a1 (Edger *et al*., 2018) with BWA-MEM (Li, 2013). The resulting SAM files were converted to BAM files, sorted and indexed using SAMtools v1.19.2 (Li *et al*., 2009). Duplicate reads were removed with Picard v3.0.0 using the 'MarkDuplicates' function (Broad Institute, 2019) and the BAM files were indexed again with SAMtools v1.19.2 (Li *et al*., 2009). Single nucleotide polymorphisms (SNPs) were called using GATK v4.5.0.0 with the 'Mutect2' function, filtered with 'FilterMutectCalls' (Van der Auwera & O'Connor, 2020) and further manually filtered to retain SNPs with an allele frequency greater than 90% and a read depth of more than ten. An *F. vesca* specific directory was built using the function 'build' and annotated with snpEff v5.2 (Cingolani *et al*., 2012).

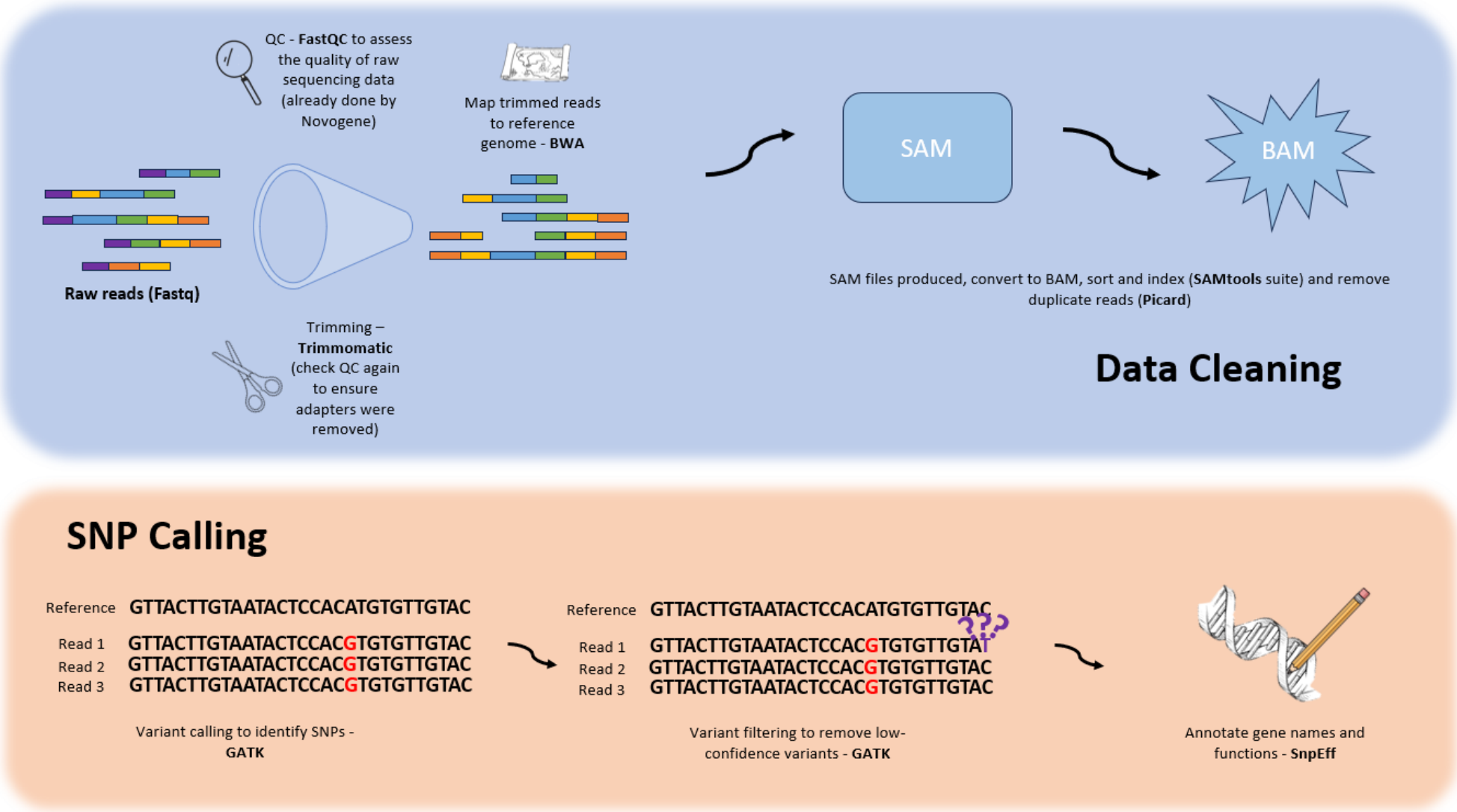


**Figure 6.** Single nucleotide polymorphism (SNP) calling pipeline and the tools utilised from raw reads to annotated SNP associated genes. Data Cleaning involved quality control (FastQC) (Andrews, 2010), trimming (Trimmomatic) (Bolger *et al*., 2014), alignment to the reference genome (BWA) (Li, 2013), and duplicate removal (SAMtools and Picard) (Li *et al*., 2009; Broad Institute, 2019). SNP Calling involved variant identification and filtering (GATK) (Van der Auwera & O'Connor, 2020), followed by annotation of gene functions (SnpEff) (Cingolani *et al*., 2012).

### 3.2.10. RNA-seq analyses

Differential expression analyses were conducted on publicly available RNA-seq data from *B. cinerea* infecting *F. vesca* leaves and non-inoculated *F. vesca* leaves, available from BioProject PRJNA818508 on NCBI (Badmi *et al*., 2022). Data processing followed the RNA-seq starter pipeline outlined on GitHub (Price, 2024): https://githu*B*.com/rj-price/rnaseq_starter. Reads were quality controlled with FastQC v0.12.0 (Andrews, 2010) pre- and post-trimming with Trimmomatic v0.39 (Bolger *et al*., 2014). Salmon v1.10.2 was then used to quantify the reads (Patro *et al*., 2017). Differential expression analysis was performed using the R package 'DESeq2' v1.38.3 (Love *et al*., 2014) and reads were annotated against the reference *F. vesca* genome v4.0.a2 (Li *et al*., 2019). SNPs that were differentially expressed during infection with *B. cinerea* were normalised, $\log_2$-transformed and visualised with the R (R Core Team, 2020) package 'pheatmap' v1.0.12 (Raivo, 2018).

### 3.2.11. Predicting candidate resistance genes

To identify candidate resistance genes for *B. cinerea* infection, genes that contained SNPs were filtered based on mutation type (Figure 7). Only mutations that resulted in missense, frameshift, splice variant, start or stop codon changes, or those labelled as high impact post-annotation were further investigated. Gene function was then examined using BLASTP (Altschul *et al*., 1990). For missense mutations, amino acid substitutions were considered more likely to cause a functional change if the amino acid group changed. Determining if the SNPs were within functional protein domains was investigated using InterPro (Paysan-Lafosse *et al*., 2023). Protein structures of genes of interest were compared to similar proteins in the AlphaFold Protein Structure Database (Jumper *et al*., 2021; Varadi *et al*., 2024). If the protein structure was at least 80% similar to the *F. vesca* protein and the amino acid was in the same position, the AlphaFold protein structure was uploaded to Missense3D to visualise whether the missense mutation was predicted to cause any 'structural damage' (Ittisoponpisan *et al*., 2019).

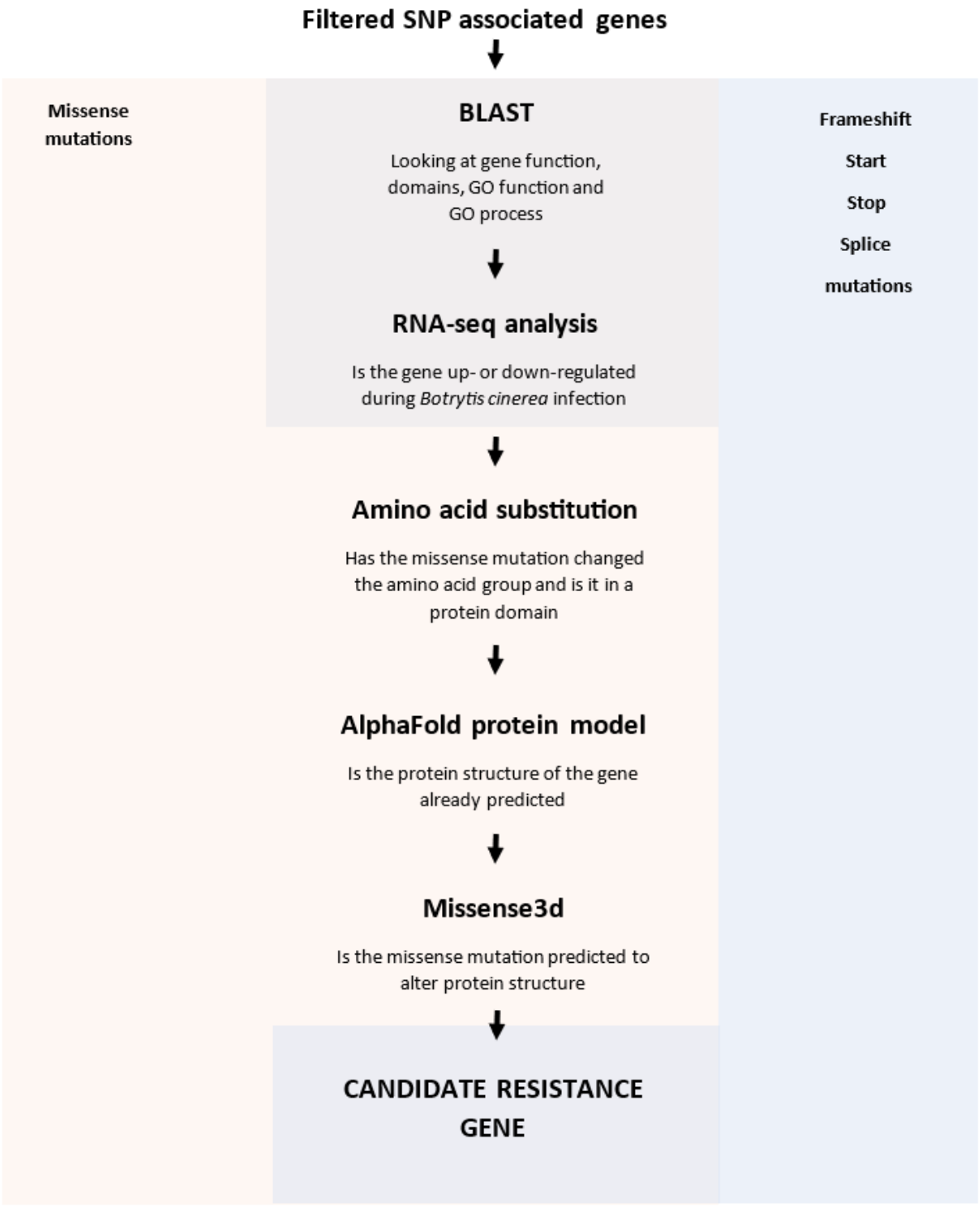


**Figure 7.** Workflow to determine candidate resistance genes for *Botrytis cinerea* infection in *Fragaria vesca* following EMS mutagenesis and SNP identification.

## 3.3. Identifying novel *B. cinerea* virulence factors

### 3.3.1. DNA extractions

To obtain material for DNA extraction a 1 cm mycelial plug, from each three-week-old isolate, was inoculated into 100 mL quarter strength potato dextrose broth and incubated for one week at 22 ˚C in the dark. The resulting mycelia were rinsed in SDW and divided into 30 mg aliquots. The mycelia were then ground to a fine powder in liquid nitrogen using a pestle and mortar and transferred into Eppendorf tubes. Following this, 500 µL of Shorty buffer [200 mM Tris-HCl pH 8.0; 400 mM LiCl; 25 mM EDTA pH 8.0; 1 % w/v SDS] was added and the samples were vortexed for 10 s. Samples were centrifuged at 16,000 *g* for 5 min and 350 µL of the supernatant was added to 350 µL isopropanol in new Eppendorf tubes and inverted for 30 s. The samples were centrifuged for 15 min at 16,000 *g* and the supernatant was carefully removed before adding 500 µL 70% ethanol. Lastly, each sample was centrifuged for 2 min at 10,000 *g*, the supernatant was removed, and the pellets were left to dry at 37 ˚C for 15 min before being resuspended in 30 µL TE buffer pH 8.0 [0.5 ml of 1M Tris-HCl pH 8.0; 0.1 ml of 0.5 M EDTA; 50 ml SDW]. DNA quality was assessed using a NanoDrop™ OneC Microvolume UV-Vis Spectrophotometer and the concentration was verified on an Invitrogen™ Qubit™ 3 Fluorometer. Samples were sent for sequencing if the OD260/280 = 1.8-2.0, the OD260/230 ≥ 1.6 and they had a concentration of ≥ 10 ng/µL.

### 3.3.2. DNA sequencing

Once sent to Novogene the extracted DNA underwent quality control, library preparation and sequencing using the Illumina NovaSeq 6000 platform with a paired-end 150 bp read length, generating approximately 5 Gb of data and 119x predicted coverage per isolate.

### 3.3.3. *De novo* genome assemblies

Raw sequencing data underwent quality control checks using FastQC v0.12.0 (Andrews, 2010) pre- and post-trimming and adapter removal with Trimmomatic v0.39 (Bolger *et al*., 2014). The trimmed reads were then subjected to *de novo* assembly using SPAdes v3.15.5 (Bankevich *et al*., 2012) and the quality of the assembled genomes were checked by searching for Leotiomycetes BUSCO with BUSCO v5.2.2 (Simão *et al*., 2015). Coverage was determined using the ‘depth’ function from SAMtools v1.19.2 (Li *et al*., 2009) and ‘comp’ and ‘plot spectra-cn’ functions from kat v2.4.2 (Mapleson *et al*., 2017). Repeats were identified and masked using RepeatModeler v2.0.5 (Flynn *et al*., 2020) and RepeatMasker v4.1.6 (Smit *et al*., 2015). Publicly available RNA-seq datasets (Table 1) were aligned to indexed repeat masked genomes with HISAT2 v2.2.1 (Kim *et al*., 2019). BRAKER v3.0.0 was used to annotate the masked genomes using the RNA-seq alignments previously mentioned, the protein databases

available on NCBI for *B. cinerea* (Table 2 & Table 3) and the existing AUGUSTUS '*Botrytis_cinerea*' species file (Gabriel *et al*., 2024; Stanke *et al*., 2008). The quality of the annotated genomes were checked again by searching for Leotiomycetes BUSCO with BUSCO v5.2.2 and the -proteome flag (Simão *et al*., 2015).

**Table 2.** List of RNA-seq sequence read archive (SRA) runs aligned to *de novo* assembled *Botrytis cinerea* genomes.

| NCBI BioProject | SRA run | Condition |
|---|---|---|
| PRJNA756518 | SRR15622386 | *Trichoderma atroviride* IMI206040 and *B. cinerea* B05.10 on PDA |
| PRJNA955032 | SRR24174271 | *B. cinerea* B05.10 mycelium 6 hrs post alpha-tomatine treatment |
| PRJNA956473 | SRR24287515 | *B cinerea* lhm-1 during sporulation |
| PRJNA1013336 | SRR26081708 | *Lactuca sativa* 33 hpi with *B. cinerea* |
| PRJNA921825 | SRR26787398 | *B. cinerea* B05.10 Bcgbl1 mutant on PDA |
| PRJNA1099710 | SRR28646870 | *B. cinerea* TG-1 after treatment of volatile organic compounds produced by *Pseudomonas chlororaphis* ZL3 |

**Table 3.** List of *Botrytis cinerea* assemblies' protein sequences downloaded from NCBI for genome annotations.

| Assembly | Isolate |
|---|---|
| GCA_000227075.1 | T4 |
| GCA_000349525.1 | BcDW1 |
| GCA_031205075.2 | M3a |
| GCA_037039525.1 | BC448 |
| GCA_037039555.1 | BC371 |
| GCF_000143535.2 | B05.10 |

#### 4.3.6. Identifying secreted effectors

The annotated proteins were extracted from the BRAKER3 gff3 output files using gffread v0.12.7 (Pertea & Pertea, 2020) and proteins containing signal peptides were predicted with SignalP 6.0 (Teufel *et al*., 2022). Proteins containing signal peptides were then analysed using EffectorP-3.0 to determine if they could be effectors. EffectorP-3.0 predicts effector proteins by identifying characteristics, such as a higher proportion of positively charged amino acids in cytoplasmic effectors and an enrichment of cysteine residues in apoplastic effectors (Sperschneider & Dodds, 2022). Orthofinder v2.5.5 was applied to determine which secreted effectors were orthologous across isolates and which were unique to each isolate (Emms & Kelly, 2019). Predicted secreted effector function was investigated using BLASTP (Altschul *et al*., 1990).

# 4. Results

## 4.1. Developing pathogenicity assays

#### 4.1.1. Pathogenicity experiments

Pathogenicity assays were designed to elucidate if *B. cinerea* has any host or organ infection specificity. Statistically significant differences were observed in disease levels between inoculated samples and the non-inoculated controls for all pathogenicity assays (Table 4). Post-hoc analyses show where the differences lie within isolate aggressiveness, with 21024 being the most aggressive in *F. vesca* leaves and flower pathogenicity experiments, 21010 being most aggressive in the *N. benthamiana* leaf pathogenicity experiment and Bc19 consistently being the least aggressive isolate across all pathogenicity assays except strawberry fruit where there was no difference in aggressiveness between isolates (Figure 8-11).

**Table 4.** Kruskal-Wallis rank sum test of *Botrytis cinerea* pathogenicity tests.

| Pathogenicity test | *H* test statistic | Degrees of freedom | *p*-value |
|---|---|---|---|
| *F. vesca* leaves | 183.08 | 10 | 2.2e-16 |
| *N. benthamiana* leaves | 60.244 | 4 | 2.578e-12 |
| *F.* × *ananassa* fruits | 126.61 | 4 | 2.2e-16 |
| *F. vesca* flowers | 67.352 | 3 | 1.574e-14 |

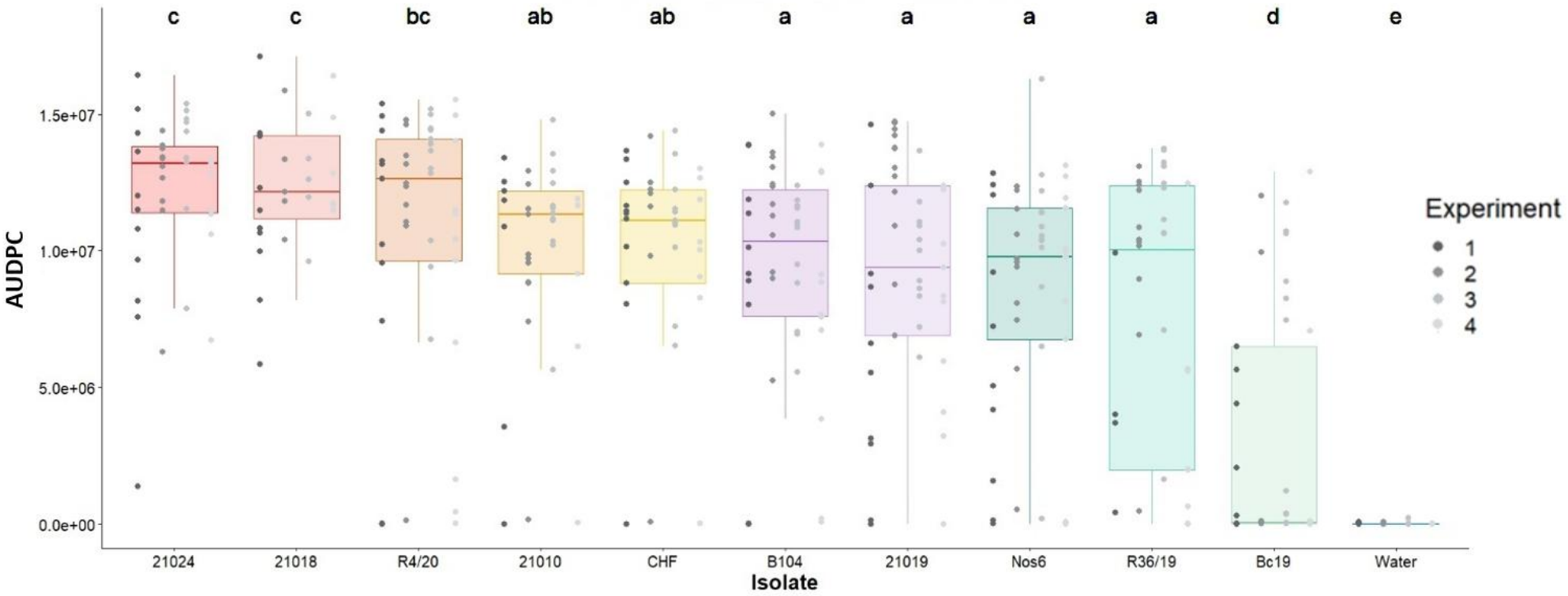


**Figure 8.** Area under the disease progression curve (AUDPC) for *Botrytis cinerea* isolates infecting *Fragaria vesca* leaf discs. Lesion development was recorded daily and analysed through image analysis. A Kruskal-Wallis rank sum test and a post-hoc Dunn Test, with the Benjamini-Hochberg method was conducted to compare isolates. Letters denote significance groupings.

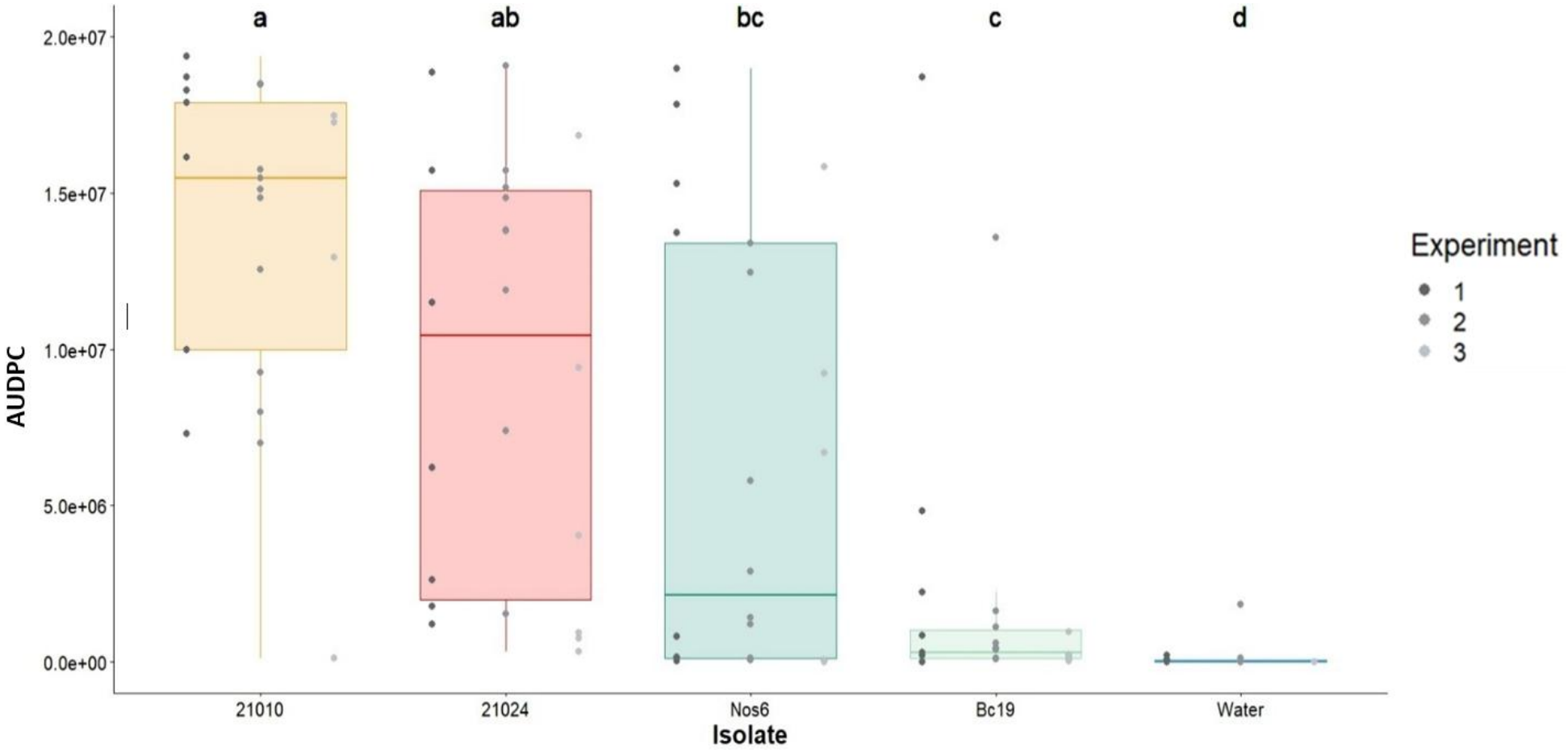


**Figure 9.** Area Under the Disease Progression Curve (AUDPC) for *Botrytis cinerea* isolates infecting *Nicotiana benthamiana* leaf discs. A Kruskal-Wallis rank sum test and a post-hoc Dunn Test, with the Benjamini-Hochberg method was conducted to compare isolates. Letters denote significance groupings.

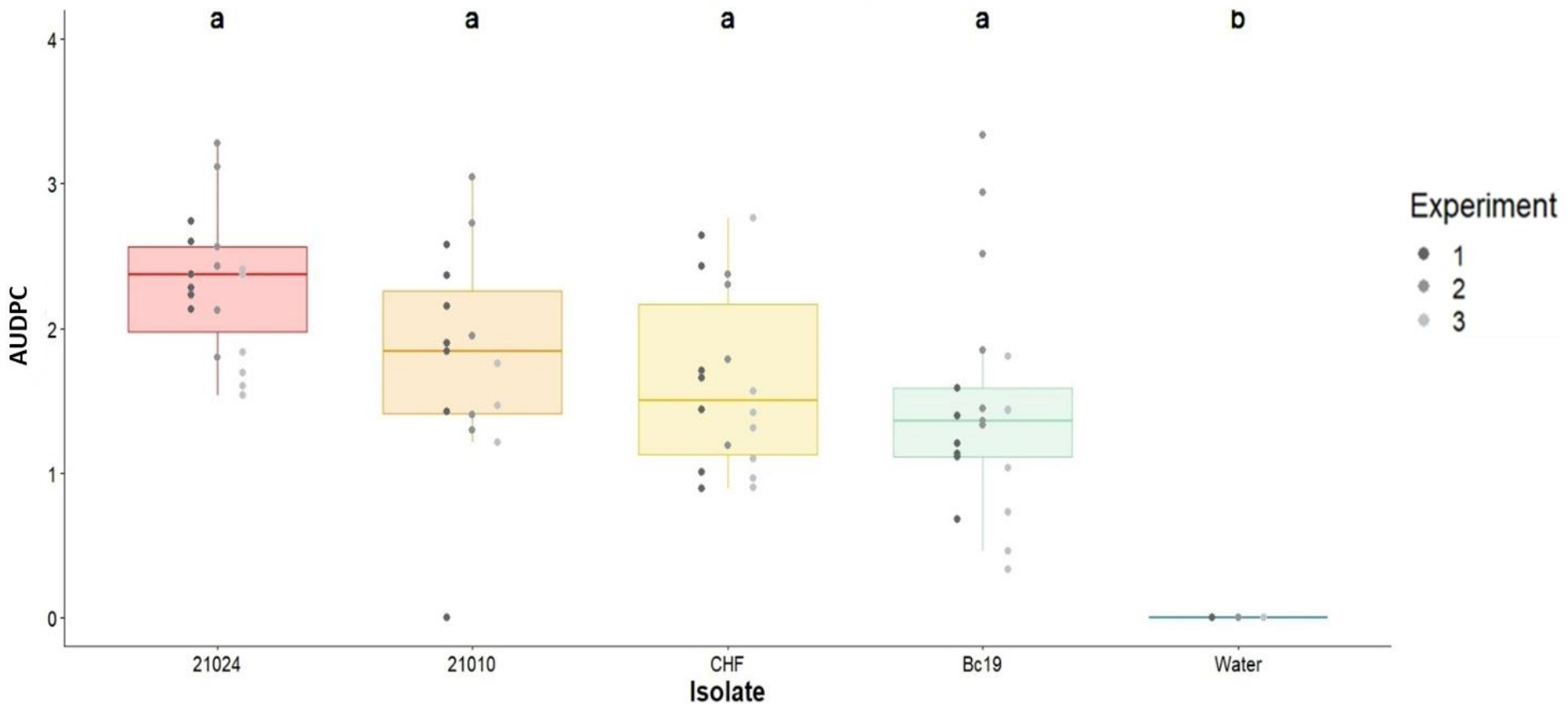


**Figure 10.** Area Under the Disease Progression Curve (AUDPC) for *Botrytis cinerea* isolates infecting *Fragaria* × *ananassa* cv. Malling Centenary fruits. A Kruskal-Wallis rank sum test and a post-hoc Dunn Test, with the Benjamini-Hochberg method was conducted to compare isolates. Letters denote significance groupings.

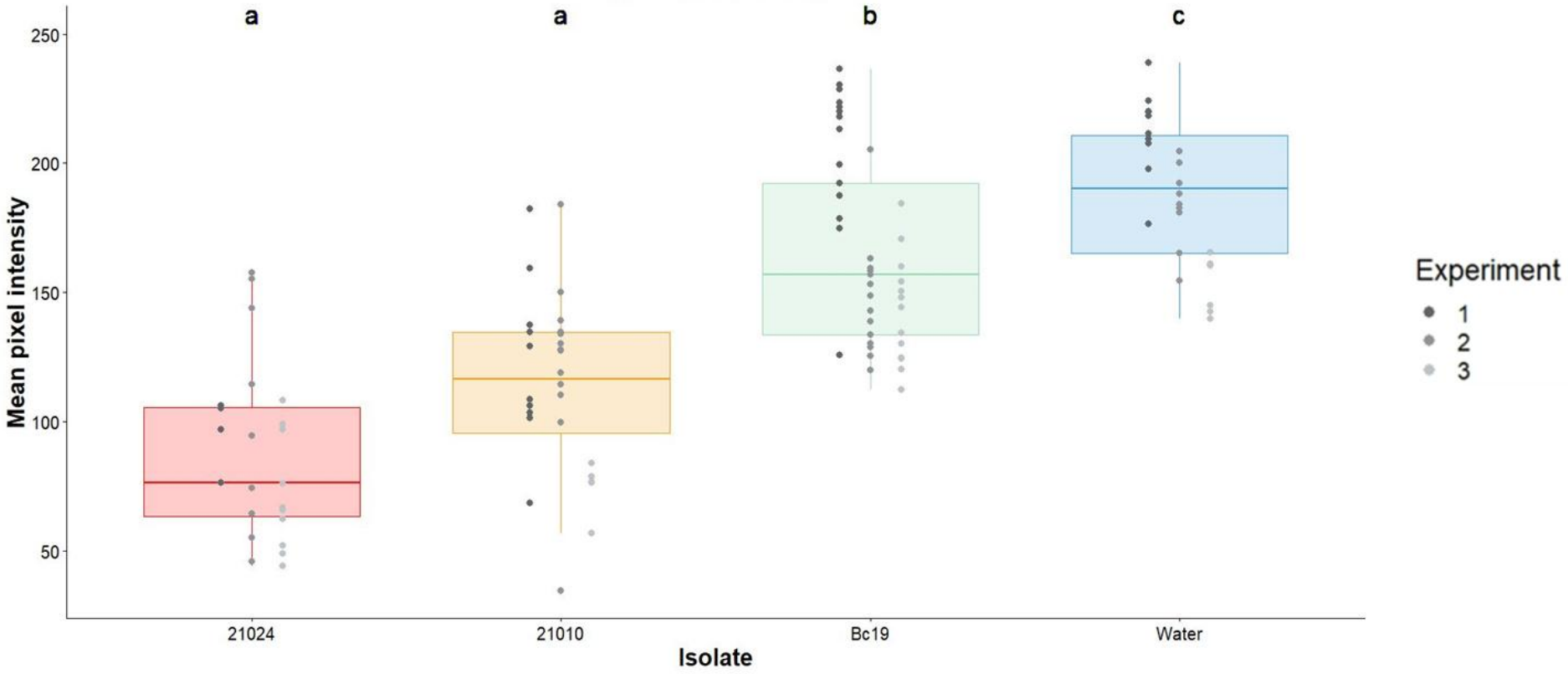


**Figure 11.** Mean pixel intensity for *Botrytis cinerea* isolates infecting *Fragaria vesca* flower stamens. A Kruskal-Wallis rank sum test and a post-hoc Dunn Test, with the Benjamini-Hochberg method was conducted to compare isolates. Letters denote significance groupings.

## 4.2. Identifying novel strawberry resistance factors

### 4.2.1. EMS mutagenesis of *Fragaria vesca* achenes

To deduce the efficacy of mutagenesis, the total number of plants exhibiting chlorotic sectoring was recorded and updated weekly. The percentage of plants displaying sectoring was 8.4% and 13.4% for treatments three (0.4% for 4 h) and four (0.4% for 8 h), respectively. In contrast, no sectoring was observed in the control plants. Chlorotic sectoring appeared in a variety of colours, most commonly yellow and pale green; however, white sectoring was seen several times (Figure 12.B-D). Additionally, abnormal leaf shapes were observed (Figure 12.E-F). The $M_2$ generation consisted of 380 plants with 21.1% of plants exhibiting mutations in sepal, flower and leaf morphology, leaf colour and variegation, fruit colour, leaf size, and plant architecture (Figure 13).

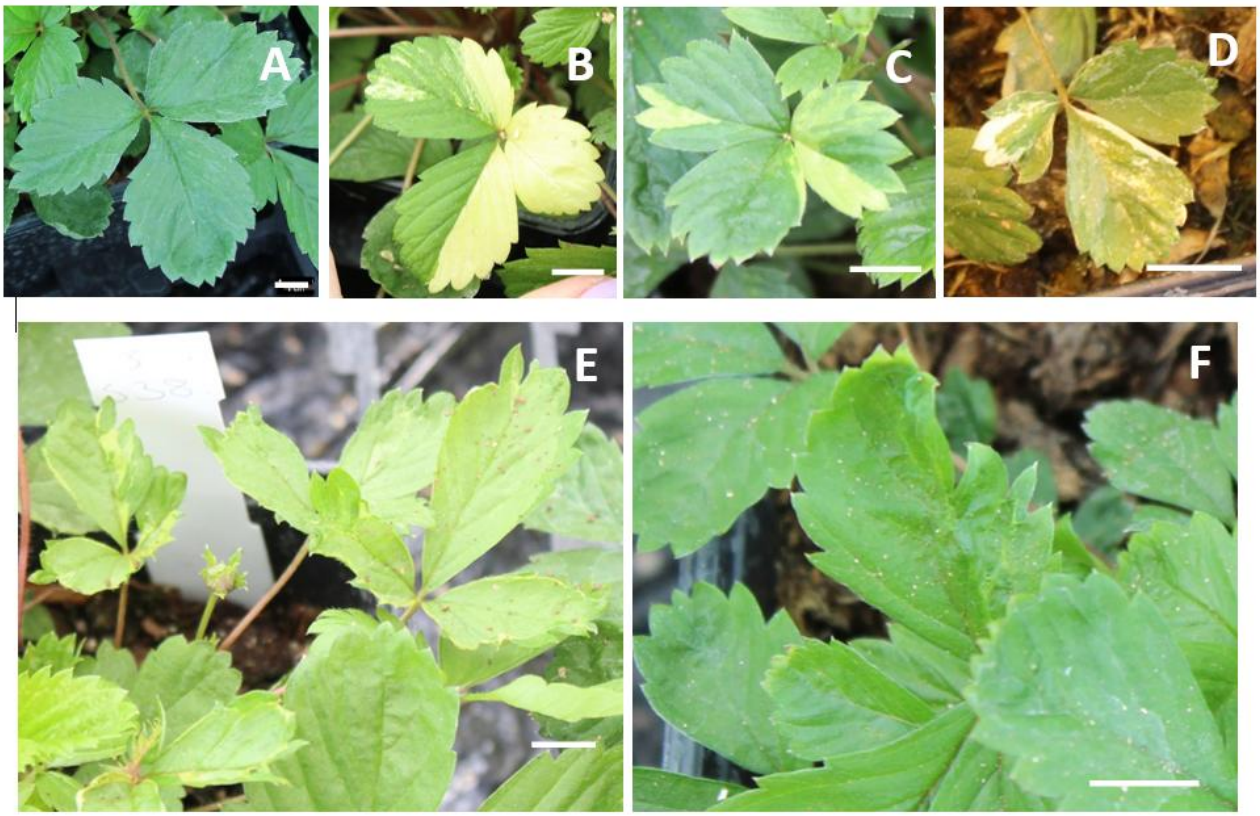


**Figure 12.** Example leaf phenotypes of *Fragaria vesca* $M_1$ mutant population. (**A**) Wild type, (**B-C**) yellow sectoring, (**D**) white sectoring, (**E-F**) abnormal leaf shapes. White scale bars in bottom right of each image are 1 cm.

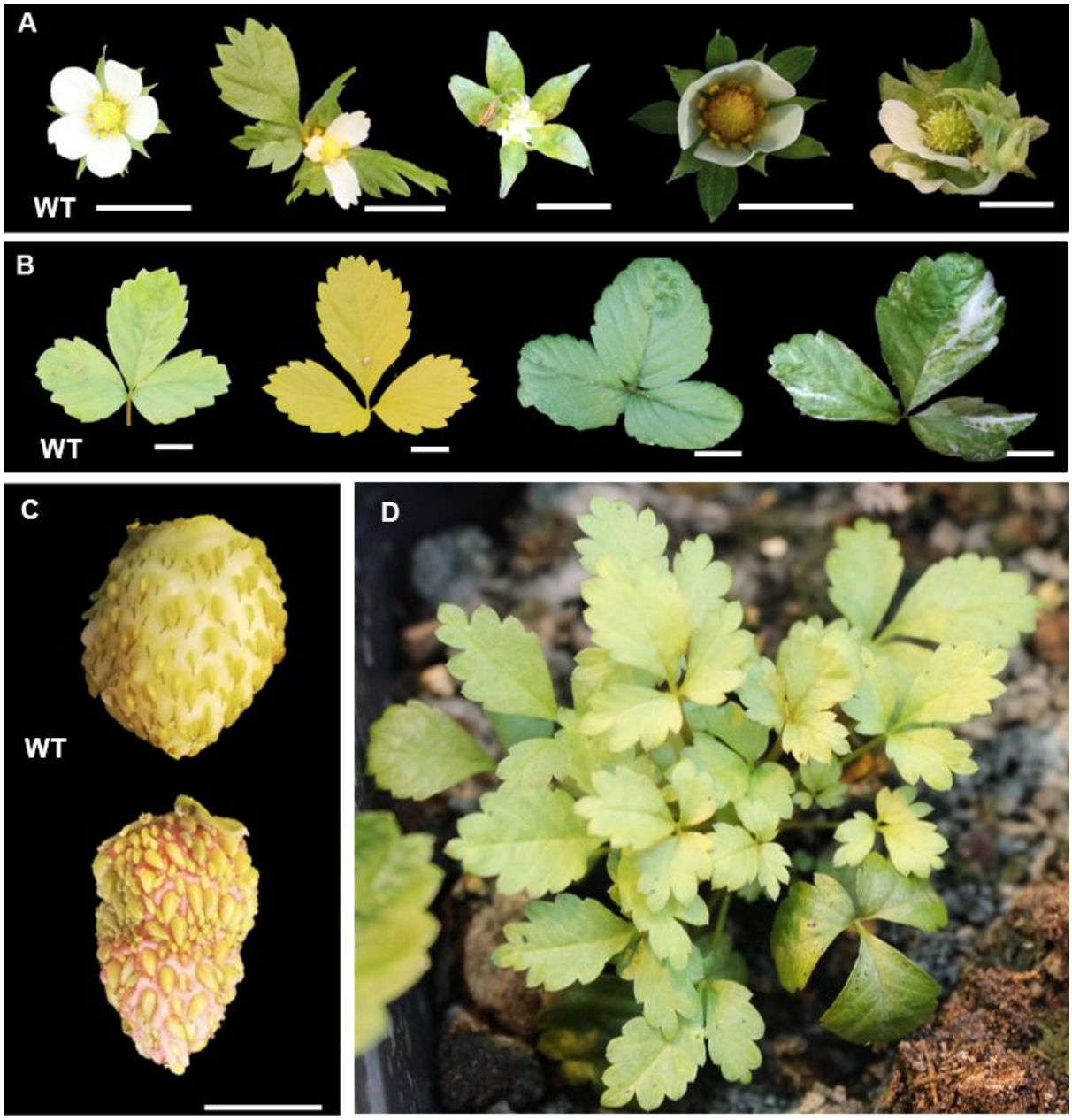


**Figure 13.** Examples of mutant (**A**) flower, (**B**) leaf colour, (**C**) fruit colour and (**D**) plant architecture phenotypes observed in an ethyl methanesulfonate $M_2$ generation of *Fragaria vesca.* White scale bars in the bottom right of each image are 1 cm.

### 4.2.2. Image analysis

The Dishy software successfully ordered the leaf discs on a Petri dish and differentiated brown lesions from healthy tissue (Figure 14).

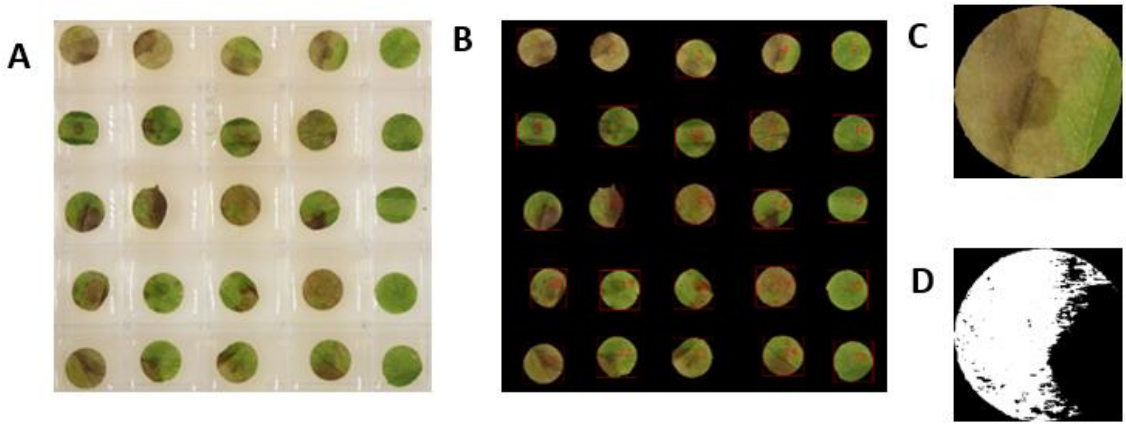


**Figure 14.** Example outputs from the Dishy software: (**A**) input image of the pathogenicity assay, (**B**) leaf discs segmented and ordered, (**C-D**) example of leaf disc number 4 and how Dishy isolates lesions, highlighting lesions in white.

### 4.2.3. Statistical analyses

Through the DRC analyses thirteen plants were found to be more statistically susceptible to *B. cinerea* infection than the WT plants (Figure 15 & Table 5). These thirteen plants were more susceptible than the WT plants at differing points along the disease progression timeline. Some plants were more susceptible than the WT plants throughout the whole infection process, such as mutants 3-128-4, 3-143-1, 3-152-1 and 4-068-1, whereas other plants were more susceptible during the initial stages of infection, such as 3-203-2, 4-006-2 ($T_{30}$) 3-070-4, 3-145-1, 3-155-1, 3-187-3 and 4-001-4 ($T_{30}$, $T_{50}$, $T_{70}$), or during the end stages of infection like 3-159-4 ($T_{50}$, $T_{70}$, $T_{90}$). One mutant, 4-068-3 ($T_{50}$), was more susceptible only during the middle stage of infection (Table 3.6). A bimodal infection pattern was observed with most mutants having either fully infected or non-infected leaf discs at day 14.

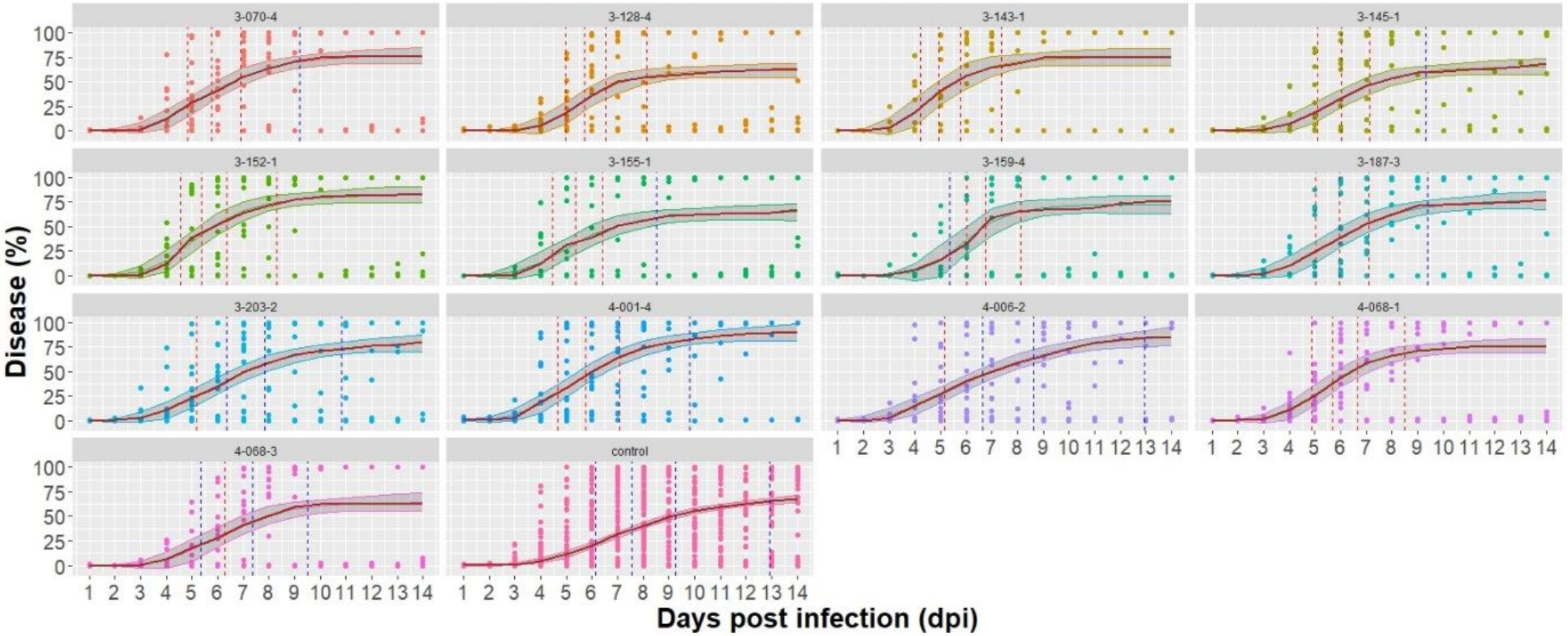


**Figure 15.** Percentage disease of ethyl methanesulfonate (EMS) *Fragaria vesca* leaf discs infected with *Botrytis cinerea* over 14 days. The numbers are the names of the individual mutants. The brown line indicates the mean percentage of the raw data and the coloured line per individual indicates the predicted values based on a log-logistic three-parameter dose response curve model. The points are the raw data, with 20 replicates per timepoint per mutant. The vertical dotted lines reference where the $T_{30}$, $T_{50}$, $T_{70}$ and $T_{90}$ values lie and are coloured in red if they are statistically significantly different from the non-mutated wild-type control plants or blue if they do not differ in significance.

**Table 5.** Significant *T* values for ethyl methanesulfonate (EMS) *Fragaria vesca* leaf discs infected with *Botrytis cinerea* against wild type control *F. vesca* leaf discs infected with *B. cinerea.*

| Mutant Comparison | *T* value | Estimate | Standard error | *t*-value | *p*-value | Adjusted *p*-value |
|---|---|---|---|---|---|---|
| 3-070-4/control | 30 | 0.785767 | 0.056699 | -3.77844 | 0.0001587 | 0.0009900 |
| 3-070-4/control | 50 | 0.764952 | 0.057769 | -4.06875 | 0.0000476 | 0.0002245 |
| 3-070-4/control | 70 | 0.74469 | 0.080789 | -3.1602 | 0.0015813 | 0.0074547 |
| 3-128-4/control | 30 | 0.81499 | 0.061898 | -2.989 | 0.0028059 | 0.0132471 |
| 3-128-4/control | 50 | 0.758158 | 0.056191 | -4.30393 | 0.0000169 | 0.0001118 |
| 3-128-4/control | 70 | 0.70529 | 0.075429 | -3.9071 | 0.0000940 | 0.0007755 |
| 3-128-4/control | 90 | 0.628573 | 0.11549 | -3.21611 | 0.0013036 | 0.0135565 |
| 3-143-1/control | 30 | 0.68989 | 0.061361 | -5.0538 | 0.0000004 | 0.0000146 |
| 3-143-1/control | 50 | 0.654973 | 0.055285 | -6.24086 | 0.0000000 | 0.0000000 |
| 3-143-1/control | 70 | 0.62182 | 0.073144 | -5.1703 | 0.0000002 | 0.0000066 |
| 3-143-1/control | 90 | 0.572436 | 0.114515 | -3.7337 | 0.0001897 | 0.0062614 |
| 3-145-1/control | 30 | 0.83287 | 0.064318 | -2.5984 | 0.0093786 | 0.0343933 |
| 3-145-1/control | 50 | 0.79989 | 0.064903 | -3.08323 | 0.0020533 | 0.0067757 |
| 3-145-1/control | 70 | 0.76821 | 0.091908 | -2.522 | 0.0116860 | 0.0385638 |
| 3-152-1/control | 30 | 0.74131 | 0.053274 | -4.8558 | 0.0000012 | 0.0000201 |
| 3-152-1/control | 50 | 0.712411 | 0.053442 | -5.38131 | 0.0000001 | 0.0000012 |
| 3-152-1/control | 70 | 0.68464 | 0.073766 | -4.2751 | 0.0000193 | 0.0003185 |
| 3-152-1/control | 90 | 0.642611 | 0.115918 | -3.08313 | 0.0020540 | 0.0135565 |
| 3-155-1/control | 30 | 0.73198 | 0.067419 | -3.9754 | 0.0000708 | 0.0005841 |
| 3-155-1/control | 50 | 0.711332 | 0.066125 | -4.36549 | 0.0000128 | 0.0001057 |
| 3-155-1/control | 70 | 0.69127 | 0.091661 | -3.3682 | 0.0007595 | 0.0041773 |
| 3-159-4/control | 50 | 0.797127 | 0.057106 | -3.55259 | 0.0003832 | 0.0015808 |
| 3-159-4/control | 70 | 0.7277 | 0.074563 | -3.652 | 0.0002615 | 0.0017259 |
| 3-159-4/control | 90 | 0.629352 | 0.113303 | -3.27131 | 0.0010742 | 0.0135565 |
| 3-187-3/control | 30 | 0.81776 | 0.063136 | -2.8865 | 0.0039042 | 0.0160875 |
| 3-187-3/control | 50 | 0.791607 | 0.063591 | -3.27709 | 0.0010524 | 0.0038589 |
| 3-187-3/control | 70 | 0.76629 | 0.089634 | -2.6074 | 0.0091376 | 0.0335045 |
| 3-203-2/control | 30 | 0.84748 | 0.061907 | -2.4638 | 0.0137650 | 0.0455400 |
| 4-001-4/control | 30 | 0.76413 | 0.051713 | -4.5612 | 0.0000051 | 0.0000567 |
| 4-001-4/control | 50 | 0.763019 | 0.05753 | -4.11923 | 0.0000383 | 0.0002108 |
| 4-001-4/control | 70 | 0.76191 | 0.085358 | -2.7893 | 0.0052926 | 0.0218320 |
| 4-006-2/control | 30 | 0.83992 | 0.068577 | -2.3344 | 0.0195970 | 0.0588000 |
| 4-068-1/control | 30 | 0.79442 | 0.054857 | -3.7476 | 0.0001795 | 0.0009900 |
| 4-068-1/control | 50 | 0.754302 | 0.052038 | -4.72152 | 0.0000024 | 0.0000261 |
| 4-068-1/control | 70 | 0.71621 | 0.070654 | -4.0166 | 0.0000595 | 0.0006545 |
| 4-068-1/control | 90 | 0.659458 | 0.110238 | -3.08915 | 0.0020128 | 0.0135565 |
| 4-068-3/control | 50 | 0.830409 | 0.070815 | -2.39483 | 0.0166464 | 0.0499391 |

### 4.2.4. Variant calling

Of the mutations analysed, the majority were missense mutations, followed by splice variants, introduction of stop or start codons and frameshift mutations (Table 6).

**Table 6.** Total SNPs and their mutation types for *Fragaria vesca* EMS mutants.

| Mutant | Total SNPs | Missense | Frameshift | High impact | Splice variant | Stop introduced | Start introduced |
|---|---|---|---|---|---|---|---|
| 3_070_4 | 92 | 15 | 0 | 1 | 1 | 0 | 0 |
| 3_128_4 | 300 | 51 | 0 | 2 | 3 | 2 | 0 |
| 3_143_1 | 308 | 46 | 1 | 4 | 6 | 1 | 0 |
| 3_145_1 | 309 | 38 | 0 | 1 | 3 | 1 | 0 |
| 3_146_1 | 112 | 16 | 0 | 2 | 0 | 2 | 0 |
| 3_152_1 | 171 | 17 | 0 | 3 | 2 | 2 | 0 |
| 3_155_1 | 188 | 25 | 0 | 4 | 5 | 0 | 1 |
| 3_159_4 | 267 | 36 | 0 | 3 | 4 | 2 | 0 |
| 3_187_3 | 133 | 25 | 1 | 4 | 3 | 3 | 0 |
| 3_203_2 | 267 | 38 | 0 | 0 | 3 | 0 | 0 |
| 4_001_1 | 513 | 77 | 1 | 9 | 6 | 6 | 0 |
| 4_006_2 | 505 | 58 | 1 | 5 | 7 | 4 | 0 |
| 4_068_1 | 823 | 108 | 0 | 11 | 14 | 6 | 0 |
| 4_068_3 | 470 | 70 | 0 | 3 | 10 | 1 | 0 |
| **Total** | **4458** | **620** | **4** | **52** | **67** | **30** | **1** |

### 4.2.5. RNA-seq analyses

RNA-seq data was obtained from BioProject PRJNA818508 on NCBI (Badmi *et al*., 2022). An example plot of SNP associated genes that were significantly differentially expressed in a mutant plant is displayed in Figure 16.

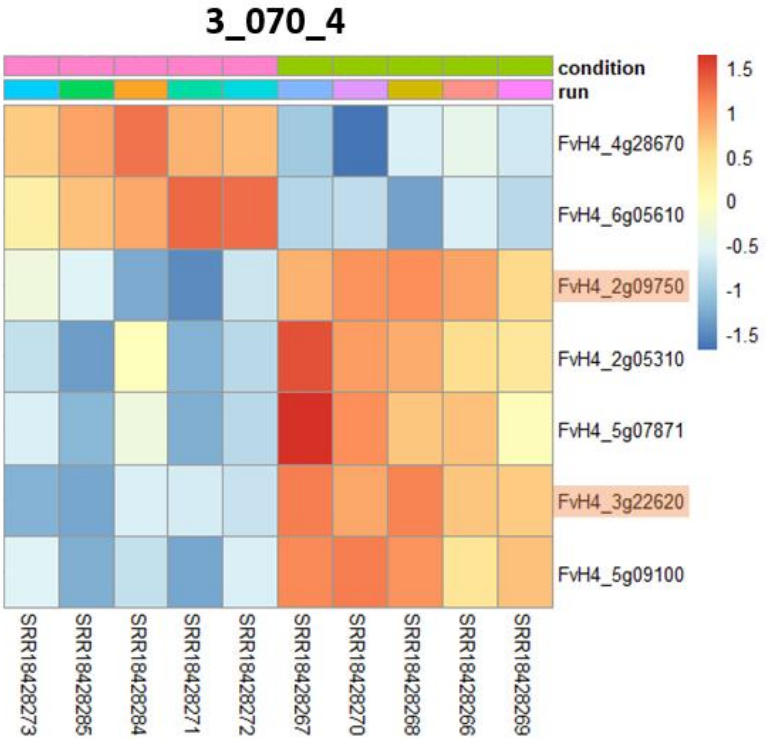


**Figure 16.** Heatmap displaying significantly differentially expressed *Fragaria vesca* genes during *Botrytis cinerea* infection of *F. vesca* leaves against water inoculated leaves, green and pink condition, respectively. Red and blue signify up or down regulated genes respectively. Data was obtained from BioProject PRJNA818508 on NCBI (Badmi *et al*., 2022). Genes highlighted in orange are candidate genes of interest.

### 4.2.6. Predicting candidate resistance genes

Of the mutations that were predicted to induce protein structural damage, five out of six involved glycine (Gly) being replaced with another amino acid (Figure 17).

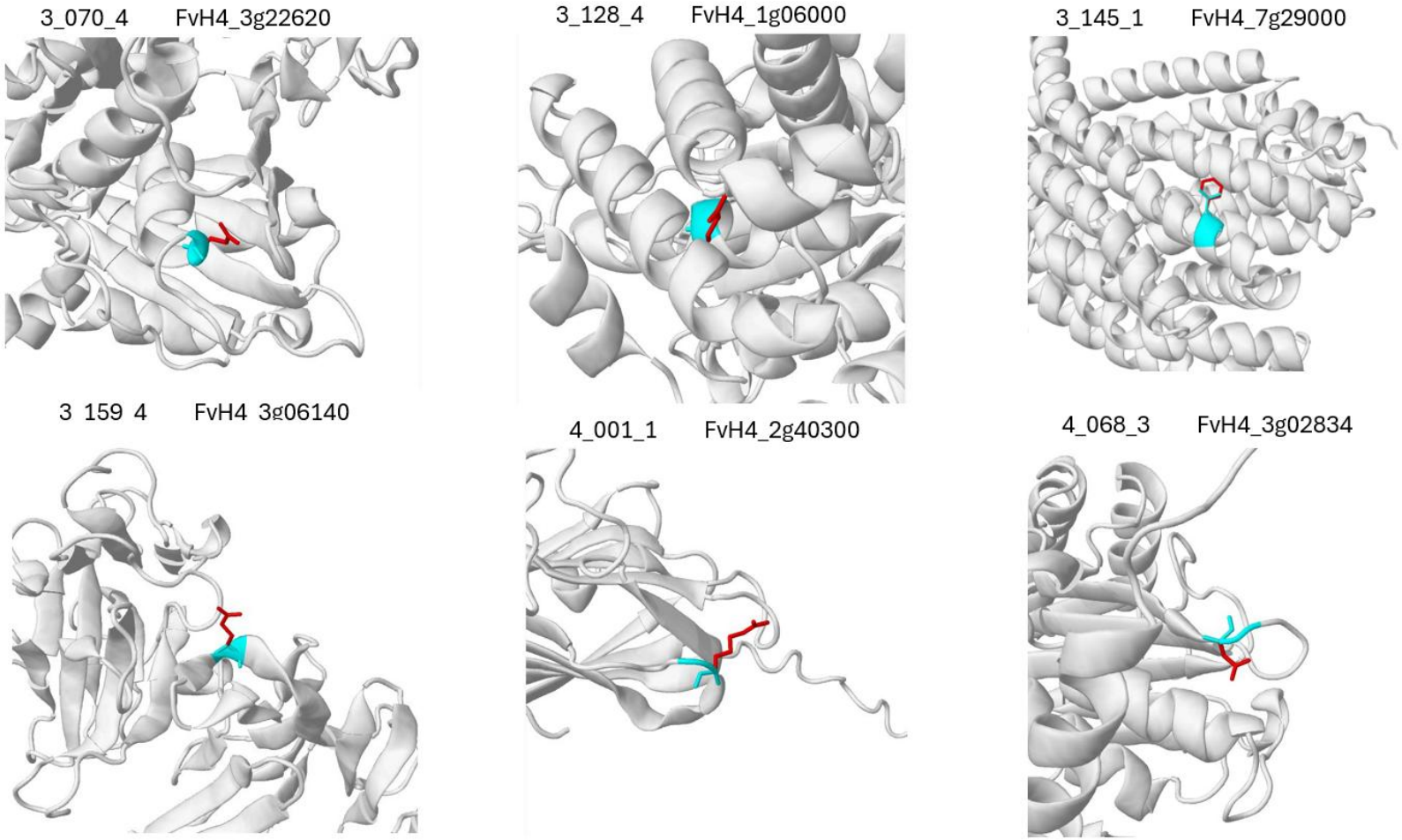


**Figure 17.** Protein structures for six candidate *Fragaria vesca* genes involved in resistance to *Botrytis cinerea* and the predicted structural changes associated with missense mutations, with blue and red representing the wild type and mutant amino acids respectively. Images obtained from Missense3D (Ittisoponpisan *et al*., 2019)

## 4.3. Identifying novel *B. cinerea* virulence factors

### 4.3.1 *De novo* genome assemblies

The genome assemblies of the *B. cinerea* isolates were analysed for key assembly metrics, including genome size, scaffold number, GC content, $N_{50}$, and $L_{50}$ (Table 7). The size of the assembled genomes ranged from approximately 41.75 Mb to 42.55 Mb. Scaffold numbers varied significantly, ranging from 1,551 in Nos6 to 264 in Bc21018, with mean scaffold sizes of 27,432 bp and 159,893 bp, respectively. The GC content was between 41.96-42.17%. The $N_{50}$ values ranged from 303,499 bp to 600,424 bp and the percentage of gaps in the assemblies were minimal, ranging from 0.0-0.01%. All assembled genomes had high sequencing depths between 133.711x and 227.811x (Table 7). The assembled genomes possessed 97.9-98.2% Leotiomycete BUSCOs indicating high levels of completeness (Table 8). The quality of the BRAKER annotated genomes was assessed using BUSCO, revealing a high level of completeness with isolates containing 99.6-99.8% Leotiomycete BUSCO proteins (Table 9).

**Table 7.** Statistics for *Botrytis cinerea de novo* assembled genomes using SPAdes (Bankevich *et al.,* 2012), such as: the size of the assembled genomes with and without ambiguous bases (Ns), scaffold number, the mean scaffold size and the range of size. GC (%) indicates the proportion of guanine and cytosine bases. $N_{50}$ and $N_{90}$ represent the scaffold lengths at which 50% and 90% of the total assembly size is reached, respectively. $L_{50}$ is the minimum number of scaffolds required to reach $N_{50}$. Gap (%) represents unsequenced regions. The average sequencing depth represents the average number of times each base in the genome is sequenced using SAMtools (Li *et al.,* 2009).

| Isolate | Size of assembled genome including Ns | Size of assembled genome without Ns | Scaffold number | Mean scaffold size | Longest scaffold sequence | Shortest scaffold sequence | GC (%) | $N_{50}$ | $L_{50}$ | $N_{90}$ | Gap (%) | Sequencing depth |
|---|---|---|---|---|---|---|---|---|---|---|---|---|
| B104 | 41,927,167 | 41,925,183 | 387 | 108,338 | 2,059,970 | 128 | 42.11 | 477,151 | 27 | 136,315 | 0.0 | 148.072 |
| Bc19 | 42,163,538 | 42,161,849 | 914 | 46,130 | 2,227,767 | 128 | 42.14 | 368,131 | 36 | 107,426 | 0.0 | 149.967 |
| Bc21010 | 42,281,814 | 42,279,883 | 1374 | 30,772 | 1,493,493 | 128 | 42.04 | 439,810 | 32 | 133,076 | 0.0 | 140.324 |
| Bc21018 | 42,211,956 | 42,208,623 | 264 | 159,893 | 1,807,884 | 128 | 42.1 | 600,424 | 22 | 202,972 | 0.01 | 148.002 |
| Bc21019 | 41,745,569 | 41,743,398 | 394 | 105,953 | 1,577,444 | 128 | 42.14 | 475,437 | 28 | 117,733 | 0.01 | 144.672 |
| Bc21024 | 41,869,554 | 41,867,591 | 835 | 50,143 | 1,552,271 | 128 | 42.17 | 454,434 | 32 | 115,235 | 0.0 | 227.811 |
| CHF | 42,063,841 | 42,062,349 | 561 | 74,980 | 1,775,020 | 128 | 42.08 | 442,236 | 29 | 112,559 | 0.0 | 143.139 |
| Nos6 | 42,548,020 | 42,546,136 | 1551 | 27,432 | 1,362,710 | 128 | 42.09 | 316,198 | 41 | 94,400 | 0.0 | 133.711 |
| R36_19 | 42,186,028 | 42,184,314 | 516 | 81,755 | 1,821,168 | 128 | 42.03 | 446,032 | 27 | 133,295 | 0.0 | 161.564 |
| R4_20 | 42,483,335 | 42,481,155 | 875 | 48,552 | 846,039 | 128 | 41.96 | 303,499 | 46 | 90,858 | 0.01 | 160.908 |

**Table 8.** Leotiomycete Benchmarking Single-Copy Orthologue (BUSCO) of the *de novo* assembled *Botrytis cinerea* genomes and the reference genome B05.10.

| Isolate | Complete (%) | Complete Single-Copy (%) | Duplicated (%) | Fragmented (%) | Missing (%) |
|---|---|---|---|---|---|
| B104 | 98 | 98 | 0 | 0.5 | 1.5 |
| Bc19 | 98.1 | 98.1 | 0 | 0.5 | 1.4 |
| Bc21010 | 98.2 | 98.1 | 0.1 | 0.5 | 1.3 |
| Bc21018 | 98.2 | 98.1 | 0.1 | 0.5 | 1.3 |
| Bc21019 | 98 | 97.9 | 0.1 | 0.6 | 1.4 |
| Bc21024 | 97.9 | 97.9 | 0 | 0.6 | 1.5 |
| CHF | 98.1 | 98.1 | 0 | 0.5 | 1.4 |
| Nos6 | 98.1 | 98.1 | 0 | 0.5 | 1.4 |
| R36_19 | 98.2 | 98.1 | 0.1 | 0.5 | 1.3 |
| R4_20 | 98.2 | 98.1 | 0.1 | 0.5 | 1.3 |
| B05.10 | 98.1 | 98.1 | 0 | 0.5 | 1.4 |

**Table 9.** Leotiomycete Benchmarking Single-Copy Orthologue (BUSCO) proteins of the *de novo* assembled and annotated *Botrytis cinerea* genomes.

| Isolate | Complete | Complete SC | Duplicated | Fragmented | Missing |
|---|---|---|---|---|---|
| B104 | 99.6 | 88.3 | 11.3 | 0 | 0.4 |
| Bc19 | 99.6 | 88.7 | 10.9 | 0 | 0.4 |
| Bc21010 | 99.7 | 88.2 | 11.5 | 0 | 0.3 |
| Bc21018 | 99.7 | 88.3 | 11.4 | 0 | 0.3 |
| Bc21019 | 99.6 | 87.9 | 11.7 | 0 | 0.4 |
| Bc21024 | 99.6 | 88.2 | 11.4 | 0 | 0.4 |
| CHF | 99.6 | 88.6 | 11 | 0 | 0.4 |
| Nos6 | 99.6 | 88.7 | 10.9 | 0 | 0.4 |
| R4_20 | 99.8 | 88.2 | 11.6 | 0 | 0.2 |
| R36_19 | 99.7 | 88.4 | 11.3 | 0 | 0.3 |

### 4.3.2. Identifying secreted effectors

There were no substantial differences between the total numbers of secreted effectors (Table 10), nor with the numbers of unique secreted effectors (Table 10) pertaining to aggressiveness groupings. Following a BLASTP search, most of the unique secreted effectors were deemed to be hypothetical proteins, only three were named proteins, which are presented in Table 11.

**Table 10.** Number of predicted secreted effectors identified in *Botrytis cinerea* isolates.

| Isolate | Total secreted effectors | Number of unique secreted effectors | Number of orthologous secreted effectors |
|---|---|---|---|
| B104 | 366 | 0 | 332 |
| Bc19 | 356 | 1 | 320 |
| Bc21010 | 367 | 2 | 324 |
| Bc21018 | 357 | 3 | 324 |
| Bc21019 | 344 | 3 | 316 |
| Bc21024 | 361 | 3 | 326 |
| CHF | 356 | 3 | 321 |
| Nos6 | 355 | 0 | 322 |
| R4_20 | 362 | 1 | 331 |
| R36_19 | 374 | 2 | 337 |

**Table 11.** BLASTP results of the predicted secreted effectors unique to individual *Botrytis cinerea* isolates.

| Isolate | Query cover | Percentage identity | Accession | Description | Domain |
|---|---|---|---|---|---|
| Bc21010 | 99 | 99.68 | XP_024551531.1 | Bcmrl1 [*Botrytis cinerea* B05.10] | ATG27; Autophagy-related protein 27 |
| Bc21024 | 87 | 84.3 | TVY62510.1 | Crotonyl-CoA hydratase [*Fusarium oxysporum F.* sp. *cubense*] | |
| | 99 | 97.66 | EMR89901.1 | putative killer toxin alpha beta protein [*Botrytis cinerea* BcDW1] | |

# 5. Discussion

## 5.1. Developing pathogenicity assays

### 5.1.1. Leaf pathogenicity assay

Leaf disc assays have been implemented to investigate *B. cinerea* infection on strawberry previously, however, these assays placed discs in wells of water and used ordinal scales (Meng *et al*., 2019, 2020), and in one instance a multispectral camera (Meng *et al*., 2020). The leaf disc assay presented in this study utilised a low-cost quantitative measure for assessing aggressiveness and incorporated a water control, which was absent from published strawberry leaf disc assays and ensures observed browning is not due to prior infection or death of the leaf disc. This new method was able to quantify isolate aggressiveness, detect variation in aggressiveness between isolates and could be applied across hosts.

Three distinct aggressiveness groups were observed from the leaf pathogenicity assay; isolates 21024, 21018 and R4/20 had high aggressiveness, isolates 21010, CHF, B104, 21019, R36/19 and Nos6 had moderate aggressiveness and isolate Bc19 had low aggressiveness (Figure 8). Most of the isolates displayed moderate aggressiveness, a trend similarly observed in the literature (Acosta Morel *et al*., 2019). The leaf disc assay was also conducted on another host, *N benthamiana,* to test for host specificity among the isolates in this study. On *N. benthamiana,* 21010 displayed high aggressiveness, isolates 21024 and Nos6 displayed moderate aggressiveness; however, isolate Bc19 showed consistent low aggressiveness (Figure 9). Isolates with varying aggressiveness across hosts has also been reported in the literature (Acosta Morel *et al*., 2019). Understanding why isolate

21010 was more aggressive on *N. benthamiana* and isolate 21024 was more aggressive on *F. vesca* leaves was investigated in objective 3 of this project.

### 5.1.2. Fruit pathogenicity assay

Many strawberry fruit pathogenicty assays have been conducted previously (Bestfleisch *et al*., 2013, 2014; Mehli *et al*., 2005; Petrasch *et al*., 2022). These assays utilised a separate fruit as a control fruit, however, this may confound results as lesions observed on inoculated fruit cannot be attributed to the inoculum with absolute certainty. Post-harvest infection can often mimic lesions derived from inoculum, as shown in Figure 2.C-F. The assay presented in this study involves cutting fruit in half and inoculating one half and using the half as a control, to exclude any fruit harbouring post-harvest infection. Without the certainty of knowing if lesions observed are based on introduced inoculum, it may be necessary to include more repeats to mitigate this confounding variable.

There were no statistically significant differences between the aggressiveness of the isolates tested on *F.* × *ananassa* cv. Malling Centenary fruits (Figure 10). Whilst initially surprising, no statistically significant differences between isolate aggressiveness on strawberry fruit has been reported before (Bestfleisch *et al*., 2014).

### 5.1.3. Flower pathogenicity assay

Only one study has been conducted investigating strawberry cultivar and *B. cinerea* isolate aggressiveness, however, they investigated flower stigma infection (Bristow *et al*., 1986). The assay presented in this project uses flower stamens since these are the most readily colonised and thought to harbour latent infections (Bristow *et al*., 1986; Jarvis, 1962; Mertely *et al*., 2002). The assay uses detached flowers in order to maximise the number of samples which can be tested all the while maintaining external conditions such as temperature and humidity the same, conditions which are of known importance regarding floral infections (Bulger *et al*., 1987).

Distinctions between isolate aggressiveness were detected as a result of the floral assay. Isolates 21024 and 21010 being isolates of high aggressiveness and isolate Bc19 being an isolate of low aggressiveness (Figure 11).

## 5.2. Identifying novel strawberry resistance factors

### 5.2.1. Dose-response curve analysis

By conducting a DRC analysis, various stages of infection could be investigated, from early-stage infection, measuring the time taken for 30% of disease to develop ($T_{30}$) to the end stages of disease

by assessing the time required for 90% of disease to have occurred ($T_{90}$). Only mutants more susceptible than the non-mutated plants were identified (Figure 15), however, this is not unlike other EMS mutagenesis studies. EMS mutagenesis has led to the discovery of many genes essential for resistance to *B. cinerea* in *Arabidopsis,* whose deletion resulted in increased susceptilbity (Bessire *et al*., 2007; Coego *et al*., 2005; Tierens *et al*., 2002).

### 5.2.2. Predicting candidate resistance genes

Candidate resistance genes were chosen based on several criteria, including their predicted functions, differences in expression post *B. cinerea* infection, amino acid substitutions and structural changes to proteins. The majority of the candidate resistance factors were found to be involved in established defence pathways, including those involved with the plant hormones, jasmonic acid, salicylic acid (SA) and abscisic acid, as well as reactive oxygen species (ROS). An example of mutations that occurred within a protein family across mutants is presented.

Mutant 3_143_1 and 4_068_3

Multiple cysteine-rich receptor-like protein kinase (CRKs) were mutated in two mutants. Mutant 3_143_1 had a mutation in CRK2 and mutant 4_068_3 had mutations in CRK7 and CRK10.

CRK2 and CRK7 are both implicated in ROS responses (Idänheimo *et al*., 2014; Kimura *et al*., 2020). ROS is an essential component for inducing cell death and whilst beneficial for protecting against biotrophic fungi, cell death enables *B. cinerea* infection (Govrin & Levine, 2002). CRK2 is essential for fine-tuning the ROS response (Levine *et al*., 1994) and CRK7 is crucial for protecting the cell from apoplastic ROS (Idänheimo *et al*., 2014). Mutating CRK2 and CRK7 could have therefore led to one plant being unable to dictate the levels of ROS produced and another unable to protect itself from the ROS it was producing, thereby inducing susceptibly to *B. cinerea.*

CRK10 is involved in SA induced immunity in rice and the overexpression of CRK10 results in statistically significantly upregulated levels of pathogenisis related (PR) proteins, PR1 and PR10 (Chern *et al*., 2016). The genes of this pathway that lead to this immunity in rice have homologues in strawberry and their interactions also lead to *FaPR1* and *FaPR10* upregulation (Luo *et al*., 2024). PR10 has been directly associated with resistance to *B. cinerea* in rose and *A. thaliana* (Lee *et al*., 2012; Li *et al*., 2024). The mutation was predicted to have had a structural change (Figure 17), which implies CRK10s function could have been altered.

The role of CRK2, 7 and 10 have not been investigated in *Fragaria* species, however, nine are upregulated during *B. cinerea* infection of *Fragaria* x *ananassa* fruit (Xiong *et al*., 2018). Given CRKs roles in other host species regarding plant immunity and their differential expression in *Fragaria* species during *B. cinerea* infections, they are a promising avenue for future research.

## 5.3. Identifying novel *B. cinerea* virulence factors

### 5.3.1. Unique predicted secreted effectors

There were three unique predicted effectors which had predicted functions following a BLASTP search, one was found in the highly aggressive isolate 21010 on *N. benthamiana* and two were found in the highly aggressive isolate 21024 on *F. vesca* (Table 11).

Isolate 21010

The predicted secreted protein in isolate 21010 was a Mannose 6-phosphate receptor-like (MPR) protein (Table 11). In mammals MPRs are crucial for the formation of clathrin-coated vesicles through the recruitment of AP-1, a clathrin adapter protein (Le Borgne & Hoflack, 1997). An MPR-like protein has been identified in *B. cinerea* and found to share a much higher protein sequence homology to mammalian MPRs than *Saccharomyces cerevisiae* (Whyte & Munro, 2001). The MPR-like protein in *B. cinerea* may therefore play a role in vesicle formation as in mammals. When proteins involved in the MPR vesicle formation pathway are mutated in *B. cinerea,* avirulence is induced French bean leaves, tomatoes and apples (Calvar, 2022). However, the role of MPR-like proteins in *B. cinerea* has not yet been elucidated.

Moreover, secretory pathways could influence host-specificity. For instance, certain secretory pathways secrete particular effectors. The clathrin/AP-1 pathway secretes the cell death inducing proteins (CDIPs): glycoprotein BcEb1 (Frías *et al*., 2016), glucoamylase BcGs1 (Zhang *et al*., 2015) and xylanase BcXyn11A (Brito *et al*., 2006) as well as an oxidoreductase, all of which are involved in *B. cinerea* infection (Souibgui *et al*., 2021). Whereas when the clathrin/AP-1 machinery is disrupted, there are comparatively more cell wall degrading enzymes (CWDEs), namely pectinases: BcPG2, BcPG4, BcPG6, BcPGX1, and BcPME2 (Souibgui *et al*., 2021). *B. cinerea* is known to secrete certain CDIPs and CWDEs depending on the host (Blanco-ulate *et al*., 2014; Jeblick *et al*., 2023). These findings suggest a potential link between secretory pathway specificity and host adaptation in *B. cinerea*. The role of the MPR-like protein needs to be investigated in *B. cinerea* to ensure they do in fact regulate clathrin/AP-1 vesicle formation.

Isolate 21024

One of the predicted secreted effectors in isolate 21024 was a putative killer toxin alpha beta protein (Table 11). In yeast, killer toxin proteins are thought to kill nearby microbes, thereby giving themselves a competitive advantage (Prins & Billerbeck, 2024; Travers-Cook *et al*., 2023). Killer toxins have not been investigated in *B. cinerea,* however, the other proteins that did not yield 'hypothetical protein' during the BLASTP search were an alpha-1,3-glucanase/mutanase from *Colletotrichum cuscutae*. Alpha-1,3-glucanase is known to degrade alpha-1,3-glucans, a vital component of some fungal cell walls. The alpha-1,3-glucanase from *Trichoderma* has anti-fungal activity (Ait-Lahsen *et al*., 2001) suggesting a similar function to killer toxin proteins from yeast.

*Crypococcus* spp. are the most abundant genera of fungi found on strawberry leaves (Abdelfattah *et al*., 2016). Furthermore, *Crypococcus* spp. have been used as biocontrol's to inhibit *B. cinerea* infection (Kowalska *et al*., 2012; Reyes-Bravo *et al*., 2022; Safitri *et al*., 2021), and alpha-1,3-glucan is a vital component of their cell walls (Reese & Doering, 2003). Isolate 21024 may have been the most virulent on strawberry leaves as it possesses this unique secreted effector which may facilitate cell wall degradation of antagonistic fungi, commonly found on strawberry leaves, thereby conferring a fitness advantage over the isolates tested.

## 6. Conclusion

Pathogenicity assays capable of determining quantitative differences in *B. cinerea* isolate aggressiveness and strawberry resistance were developed. Identifying candidate resistance factors and candidate virulence factors lays the foundation for future work. The identification of putative host resistance factors and candidate fungal effectors provides a foundation for future functional validation, resistance breeding and development of sustainable control methods.

## 7. References

Abdelfattah, A., Wisniewski, M., Nicosia, M. G. D., Cacciola, S. O., & Schena, L. (2016). Metagenomic analysis of fungal diversity on strawberry plants and the effect of management practices on the fungal community structure of aerial organs. *PLoS ONE*, *11*(8), 1–17. https://doi.org/10.1371/journal.pone.0160470

Abràmoff, M. D., Magalhães, P. J., & Ram, S. J. (2004). Image processing with imageJ. *Biophotonics International*, *11*(7), 36–42. https://doi.org/10.1201/9781420005615.ax4

Acosta Morel, W., Marques-Costa, T. M., Santander-Gordon, D., Anta Fernandez, *F.*, Zabalgogeazcoa, I., Vazquez de Aldana, *B.* R., Sukno, S. A., Dıaz-Mınguez, J. M., & Benito, E. P. (2019). Physiological and population genetic analysis of *Botrytis* field isolates from vineyards in Castilla y Leon, Spain. *Plant Pathology*, *68*, 523–536.

https://doi.org/10.1111/ppa.12967

Ait-Lahsen, H., Soler, A., Rey, M., De La Cruz, J., Monte, E., & Llobell, A. (2001). An Antifungal Exo-α-1,3-Glucanase (AGN13.1) from the Biocontrol Fungus *Trichoderma harzianum*. *Applied and Environmental Microbiology*, *67*(12), 5833–5839. https://doi.org/10.1128/AEM.67.12.5833-5839.2001

Alexa, A., & Rahnenführer, J. (2023). *topGO: Enrichment analysis for Gene Ontology*. R Package Version 2.52.0. https://bioconductor.org/packages/topGO/

Altschul, S., Gish, W., Miller, W., Myers, E. W., & Lipman, D. J. (1990). Basic local alignment search tool. *Journal of Molecular Biology*, *215*(3), 403–410.

Andrews, S. (2010). *FastQC: A quality control tool for high throughput sequence data.* https://www.bioinformatics.babraham.ac.uk/projects/fastqc/

Badmi, R., Tengs, T., Brurberg, M. *B.*, Elameen, A., Zhang, Y., Haugland, L. K., Fossdal, C. G., Hytönen, T., Krokene, P., & Thorstensen, T. (2022). Transcriptional profiling of defense responses to *Botrytis cinerea* infection in leaves of *Fragaria vesca* plants soil-drenched with beta-aminobutyric acid. *Frontiers in Plant Science*, *13*. https://doi.org/10.3389/fpls.2022.1025422

Bankevich, A., Nurk, S., Antipov, D., Gurevich, A. A., Dvorkin, M., Kulikov, A. S., Lesin, V. M., Nikolenko, S. I., Pham, S. O. N., Prjibelski, A. D., Pyshkin, A. V, Sirotkin, A. V, Vyahhi, N., Tesler, G., Alekseyev, M. A. X. A., & Pevzner, P. A. (2012). SPAdes: A New Genome Assembly Algorithm and Its Applications to Single-Cell Sequencing. *JOURNAL OF COMPUTATIONAL BIOLOGY*, *19*(5), 455–477. https://doi.org/10.1089/cm*B.*2012.0021

Bessire, M., Jacquat, A., Humphry, M., Borel, S., Macdonald-comber, J., & Nawrath, C. (2007). A permeable cuticle in *Arabidopsis* leads to a strong resistance to *Botrytis cinerea*. *The EMBO Journal*, *26*(8), 2158–2168. https://doi.org/10.1038/sj.emboj.7601658

Bestfleisch, M., Höfer, M., Richter, K., Hanke, M., Schulte, E., & Peil, A. (2013). Breeding of resistant strawberry cultivars for organic fruit production – Diallel crossing strategies and resistance tests for *Botrytis cinerea* and Xanthomonas *Fragaria*e . *Acta Horticulturae*, *976*, 221–227.

Bestfleisch, M., Luderer-Pflimpfl, M., Höfer, M., Schulte, E., Wünsche, J. N., Hanke, M. V., & Flachowsky, H. (2014). Evaluation of strawberry (*Fragaria* L.) genetic resources for resistance to *Botrytis cinerea*. *Plant Pathology*, *64*(2), 396–405. https://doi.org/10.1111/ppa.12278

Blanco-ulate, *B.*, Morales-Cruz, A., Amrine, K. C. H., Labavitch, J. M., Powell, A. L. T., & Cantu, D. (2014). Genome-wide transcriptional profiling of *Botrytis cinerea* genes targeting plant cell walls during infections of different hosts. *Frontiers in Plant Science*, *5*(September), 1–16. https://doi.org/10.3389/fpls.2014.00435

Bolger, A. M., Lohse, M., & Usadel, *B.* (2014). Genome analysis Trimmomatic: a flexible trimmer for Illumina sequence data. *Bioinformatics*, *30*(15), 2114–2120.

https://doi.org/10.1093/bioinformatics/btu170

Bristow, P. R., McNicol, R. J., & Williamson, *B.* (1986). Infection of strawberry flowers by *Botrytis cinerea* and its relevance to grey mould development. *Annals of Applied Biology*, *109*, 545–554.

Brito, N., Espino, J. J., & González, C. (2006). The endo-β-1,4-xylanase Xyn11A is required for virulence in *Botrytis cinerea*. *Molecular Plant-Microbe Interactions*, *19*(1), 25–32. https://doi.org/10.1094/MPMI-19-0025

Bulger, M. A., Ellis, M. A., & Madden, L. V. (1987). Influence of Temperature and Wetness Duration on Infection of Strawberry Flowers by *Botrytis cinerea* and Disease Incidence of Fruit Originating from Infected Flowers. *Ecology and Epidemiology*, *77*(8), 1225–1230.

Calleja, E. (2011). *The potential impacts of climate change on diseases affecting strawberries and the UK strawberry industry*.

Calvar, G. (2022). Role of the clathrin adaptor AP-1 in the virulence and the biogenesis process of secretory vesicles in the plant-pathogenic fungus *Botrytis cinerea*. In *Microbiology and Parasitology*.

Chern, M., Xu, Q., Bart, R. S., Bai, W., Ruan, D., Sze-To, W. H., Canlas, P. E., Jain, R., Chen, X., & Ronald, P. C. (2016). A Genetic Screen Identifies a Requirement for Cysteine-Rich–Receptor-Like Kinases in Rice NH1 (OsNPR1)-Mediated Immunity. *PLoS Genetics*, *12*(5), 1–20. https://doi.org/10.1371/journal.pgen.1006049

Cingolani, P., Platts, A., Wang, L. L., Coon, M., Nguyen, T., Wang, L., Land, S. J., Lu, X., & M, R. D. (2012). A program for annotating and predicting the effects of single nucleotide polymorphisms, SnpEff: SNPs in the genome of Drosophila melanogaster strain w1118 ; iso-2; iso-3. *Fly*, *6*(2), 80–92. https://doi.org/10.1070/qe1980v010n03abeh009978

Clark, M., Springmann, M., Rayner, M., Scarborough, P., Hill, J., Tilman, D., Macdiarmid, J. I., Fanzo, J., Bandy, L., & Harrington, R. A. (2022). Estimating the environmental impacts of 57,000 food products. *Proceedings of the National Academy of Sciences of the United States of America*, *119*(33). https://doi.org/10.1073/pnas.2120584119

Coego, A., Ramirez, V., Gil, M. J., Flors, V., Mauch-Mani, *B.*, & Vera, P. (2005). An *Arabidopsis* homeodomain transcription factor, overexpressor of cationic peroxidase 3, mediates resistance to infection by necrotrophic pathogens. *Plant Cell*, *17*(7), 2123–2137. https://doi.org/10.1105/tpc.105.032375

da Silva Pinto, M., de Carvalho, J. E. De, Lajolo, *F.* M., Genovese, M., & Shetty, K. (2010). Evaluation of Antiproliferative, Anti-Type 2 Diabetes, and Antihypertension Potentials of Ellagitannins from Strawberries (*Fragaria* x *ananassa* Duch.) Using In Vitro Models. *JOURNAL OF MEDICINAL FOOD*, *13*(5), 1027–1035.

Daugaard, H. (1999). Cultural methods for controlling *Botrytis cinerea* in strawberry. *Biological Agriculture and Horticulture*, *16*, 351–361. https://doi.org/10.17660/ActaHortic.2002.567.142

Dreher, M. L., & Ford, N. A. (2020). A Comprehensive Critical Assessment of Increased Fruit and Vegetable Intake on Weight Loss in Women. *Nutrients*, *12*(1919).

Edger, P. P., Vanburen, R., Colle, M., Poorten, T. J., Wai, C. M., Niederhuth, C. E., Alger, E. I., Ou, S., Acharya, C. *B.*, Wang, J., Callow, P., Mckain, M. R., Shi, J., Collier, C., Xiong, Z., Mower, J. P., Jiang, N., Childs, K. L., Slovin, J. P., … Knapp, S. J. (2018). Single-molecule sequencing and optical mapping yields an improved genome of woodland strawberry ( *Fragaria vesca* ) with chromosome-scale contiguity. *GigaScience*, *7*, 1–7. https://doi.org/10.1093/gigascience/gix124

Edmondson, R, N. (2021). *Blocksdesign: Nested and Crossed Block Designs for Factorial and Unstructured Treatment Sets*. https://cran.r-project.org/package=blocksdesign

Emms, D. M., & Kelly, S. (2019). OrthoFinder: Phylogenetic orthology inference for comparative genomics. *Genome Biology*, *20*(1), 1–14. https://doi.org/10.1186/s13059-019-1832-y

FAOSTAT. (2022). *FAOSTAT Agriculture data*. http://www.fao.org/faostat/en/#data/QC

Flynn, J. M., Hubley, R., Goubert, C., Rosen, J., Clark, A. G., Feschotte, C., & Smit, A. *F.* (2020). RepeatModeler2 for automated genomic discovery of transposable element families. *Proceedings of the National Academy of Sciences of the United States of America*, *117*(17), 9451–9457. https://doi.org/10.1073/pnas.1921046117

Frías, M., González, M., González, C., & Brito, N. (2016). BcIEB1, a *Botrytis cinerea* secreted protein, elicits a defense response in plants. *Plant Science*, *250*, 115–124. https://doi.org/10.1016/j.plantsci.2016.06.009

Gabriel, L., Brůna, T., Hoff, K. J., Ebel, M., Lomsadze, A., Borodovsky, M., & Stanke, M. (2024). BRAKER3: Fully automated genome annotation using RNA-seq and protein evidence with GeneMark-ETP, AUGUSTUS, and TSEBRA. *Genome Research*, 1–21. https://doi.org/10.1101/gr.278090.123

González, G., Moya, M., Sandoval, C., & Herrera, R. (2009). Genetic diversity in Chilean strawberry (*Fragaria chiloensis*): differential response to *Botrytis cinerea* infection. *Spanish Journal of Agricultural Research*, *7*(4), 886. https://doi.org/10.5424/sjar/2009074-1102

Govrin, E. M., & Levine, A. (2002). Infection of *Arabidopsis* with a necrotrophic pathogen, *Botrytis cinerea*, elicits various defense responses but does not induce systemic acquired resistance (SAR). *Plant Molecular Biology*, *48*(3), 267–276. https://doi.org/10.1023/A:1013323222095

Idänheimo, N., Gauthier, A., Salojärvi, J., Siligato, R., Brosché, M., Kollist, H., Mähönen, A. P., Kangasjärvi, J., & Wrzaczek, M. (2014). The *Arabidopsis* thaliana cysteine-rich receptor-like kinases CRK6 and CRK7 protect against apoplastic oxidative stress. *Biochemical and Biophysical Research Communications*, *445*(2), 457–462. https://doi.org/10.1016/j.bbrc.2014.02.013

Institute, *B.* (2019). *Picard toolkit*. Broad Institute, GitHub Repository. http://broadinstitute.githu*B*.io/picard/

Ittisoponpisan, S., Islam, S. A., Khanna, T., Alhuzimi, E., David, A., & Sternberg, M. J. E. (2019). Can Predicted Protein 3D Structures Provide Reliable Insights into whether Missense Variants Are Disease Associated? *Journal of Molecular Biology*, *431*(11), 2197–2212. https://doi.org/10.1016/j.jm*B.*2019.04.009

Jarvis, W. R. (1962). The infection of strawberry and raspberry fruits by *Botrytis cinerea* Fr. *Annals of Applied Biology*, *50*, 569–575.

Jeblick, T., Leisen, T., Steidele, C. E., Albert, I., Müller, J., Kaiser, S., Mahler, *F.*, Sommer, *F.*, Keller, S., Hückelhoven, R., Hahn, M., & Scheuring, D. (2023). *Botrytis* hypersensitive response inducing protein 1 triggers noncanonical PTI to induce plant cell death. *Plant Physiology*, *191*(1), 125–141. https://doi.org/10.1093/plphys/kiac476

Jumper, J., Evans, R., Pritzel, A., Green, T., Figurnov, M., Ronneberger, O., Tunyasuvunakool, K., Bates, R., Žídek, A., Potapenko, A., Bridgland, A., Meyer, C., Kohl, S. A. A., Ballard, A. J., Cowie, A., Romera-Paredes, *B.*, Nikolov, S., Jain, R., Adler, J., … Hassabis, D. (2021). Highly accurate protein structure prediction with AlphaFold. *Nature*, *596*(7873), 583–589. https://doi.org/10.1038/s41586-021-03819-2

Kim, D., Paggi, J. M., Park, C., Bennett, C., & Salzberg, S. L. (2019). Graph-based genome alignment and genotyping with HISAT2 and HISAT-genotype. *Nature Biotechnology*, *37*(8), 907–915. https://doi.org/10.1038/s41587-019-0201-4

Kimura, S., Hunter, K., Vaahtera, L., Tran, H. C., Citterico, M., Vaattovaara, A., Rokka, A., Stolze, S. C., Harzen, A., Meißner, L., Wilkens, M. M. T., Hamann, T., Toyota, M., Nakagami, H., & Wrzaczek, M. (2020). CRK2 and C-terminal phosphorylation of NADPH oxidase RBOHD regulate reactive oxygen species production in *Arabidopsis*. *Plant Cell*, *32*(4), 1063–1080. https://doi.org/10.1105/tpc.19.00525

Kowalska, J., Drożdżyński, D., Remlein-Starosta, D., Sas-Paszt, L., & Malusá, E. (2012). Use of Cryptococcus albidus for controlling grey mould in the production and storage of organically grown strawberries. *Journal of Plant Diseases and Protection*, *119*(5/6), 174–178.

Kretschmer, M., Leroch, M., Mosbach, A., Walker, A., Fillinger, S., Mernke, D., Schoonbeek, H., Pradier, J., Leroux, P., Waard, M. A. De, & Hahn, M. (2009). Fungicide-Driven Evolution and Molecular Basis of Multidrug Resistance in Field Populations of the Grey Mould Fungus *Botrytis cinerea*. *PLoS Pathogens*, *5*(12), 1–13. https://doi.org/10.1371/journal.ppat.1000696

Kruskal, W. H., & Wallis, W. A. (1952). Use of Ranks in One-Criterion Variance Analysis. *Journal of the American Statistical Association*, *47*(260), 583–621. https://doi.org/10.1080/01621459.1952.10483441

Kurniati, D., Kundaryanti, R., & Ericha, S. R. (2021). The Effect Fe Tablets and Vitamin C with Fe Tablets and Strawberry Juice on Hb Adolescent Girls. *Nursing and Health Sciences Journal (NHSJ)*, *1*(2), 125–129. https://doi.org/10.53713/nhs.v1i2.60

Le Borgne, R., & Hoflack, *B.* (1997). Mannose 6-phosphate receptors regulate the formation of

clathrin-coated vesicles in the TGN. *Journal of Cell Biology*, *137*(2), 335–345. https://doi.org/10.1083/jc*B.*137.2.335

Lee, O. R., Kim, Y. J., Balusamy, S. R. D., Khorolragchaa, A., Sathiyaraj, G., Kim, M. K., & Yang, D. C. (2012). Expression of the ginseng PgPR10-1 in *Arabidopsis* confers resistance against fungal and bacterial infection. *Gene*, *506*(1), 85–92. https://doi.org/10.1016/j.gene.2012.06.039

Leroch, M., Kretschmer, M., & Hahn, M. (2011). Fungicide Resistance Phenotypes of *Botrytis cinerea* Isolates from Commercial Vineyards in South West Germany. *Journal of Phytopathology*, *159*, 63–65. https://doi.org/10.1111/j.1439-0434.2010.01719.x

Levine, A., Tenhaken, R., Dixon, R., & Lamb, C. (1994). H202 from the Oxidative Burst Orchestrates the Plant Hypersensitive Disease Resistance Response. *Cell*, *79*, 583–593.

Li, H. (2013). Aligning sequence reads, clone sequences and assembly contigs with BWA-MEM. *ArXiv:1303.3997v2 [q-Bio.GN]*, *00*(00), 1–3. http://arxiv.org/abs/1303.3997

Li, H., Handsaker, *B.*, Wysoker, A., Fennell, T., Ruan, J., Homer, N., Marth, G., Abecasis, G., & Durbin, R. (2009). The Sequence Alignment/Map format and SAMtools. *Bioinformatics*, *25*(16), 2078–2079. https://doi.org/10.1093/bioinformatics/btp352

Li, R., Yao, J., Ming, Y., Guo, J., Deng, J., Liu, D., Li, Z., & Cheng, Y. (2024). Integrated proteomic analysis reveals interactions between phosphorylation and ubiquitination in rose response to *Botrytis* infection. *Horticulture Research*, *11*(1). https://doi.org/10.1093/hr/uhad238

Li, Y., Pi, M., Gao, Q., & Liu, Z. (2019). Updated annotation of the wild strawberry *Fragaria vesca* V4 genome. *Horticulture Research*. https://doi.org/10.1038/s41438-019-0142-6

Love, M. I., Huber, W., & Anders, S. (2014). Moderated estimation of fold change and dispersion for RNA-seq data with DESeq2. *Genome Biology*, *15*(12), 1–21. https://doi.org/10.1186/s13059-014-0550-8

Luo, J., Yu, W., Xiao, Y., Zhang, Y., & Peng, *F.* (2024). FaSnRK1a mediates salicylic acid pathways to enhance strawberry resistance to *Botrytis cinerea*. *Horticultural Plant Journal*, *10*(1), 131–144.

Mapleson, D., Accinelli, G. G., Kettleborough, G., Wright, J., & Clavijo, *B.* J. (2017). KAT: A K-mer analysis toolkit to quality control NGS datasets and genome assemblies. *Bioinformatics*, *33*(4), 574–576. https://doi.org/10.1093/bioinformatics/btw663

Mehli, L., Kjellsen, T. D., Dewey, *F.* M., Hietala, A. M., & Mehli, L. (2005). A case study from the interaction of strawberry and *Botrytis cinerea* highlights the benefits of comonitoring both partners at genomic and mRNA level. *New Phytologist*, *168*, 465–474.

Mendiburu, *F.*, & Yaseen, M. (2020). *agricolae: Statistical Procedures for Agricultural Research*. https://myaseen208.githu*B.*io/agricolae/https://cran.r-project.org/package=agricolae.

Meng, L., Höfte, M., & Van Labeke, M. C. (2019). Leaf age and light quality influence the basal resistance against *Botrytis cinerea* in strawberry leaves. *Environmental and Experimental*

*Botany*, *157*(September 2018), 35–45. https://doi.org/10.1016/j.envexpbot.2018.09.025

Meng, L., Van Labeke, M. C., & Höfte, M. (2020). Timing of light quality affects susceptibility to *Botrytis cinerea* in strawberry leaves. *Journal of Photochemistry and Photobiology B: Biology*, *211*(July), 111988. https://doi.org/10.1016/j.jphotobiol.2020.111988

Mertely, J. C., Mackenzie, S. J., Legard, D. E., & Road, L. G. (2002). Timing of Fungicide Applications for *Botrytis cinerea* Based on Development Stage of Strawberry Flowers and Fruit. *Plant Disease*, *86*(September), 1019–1024.

Patro, R., Duggal, G., Love, M. I., Irizarry, R. A., & Kingsford, C. (2017). Salmon: fast and bias-aware quantification of transcript expression using dual-phase inference. *Nature Methods*, *14*(4), 417–419. https://doi.org/10.1038/nmeth.4197

Paysan-Lafosse, T., Blum, M., Chuguransky, S., Grego, T., Pinto, *B.* L., Salazar, G. A., Bileschi, M. L., Bork, P., Bridge, A., Colwell, L., Gough, J., Haft, D. H., Letunić, I., Marchler-Bauer, A., Mi, H., Natale, D. A., Orengo, C. A., Pandurangan, A. P., Rivoire, C., … Bateman, A. (2023). InterPro in 2022. *Nucleic Acids Research*, *51*(D1), D418–D427. https://doi.org/10.1093/nar/gkac993

Pertea, G., & Pertea, M. (2020). GFF Utilities: GffRead and GffCompare [version 2; peer review: 3 approved]. *F1000Research*, *9*(304), 1–20. https://f1000research.com/articles/9-304/v2

Petrasch, S., Mesquida-pesci, S. D., Pincot, D. D. A., Feldmann, M. J., López, C. M., Famula, R., Hardigan, M. A., Cole, G. S., Knapp, S. J., & Blanco-ulate, *B.* (2022). Genomic Prediction of Strawberry Resistance to Postharvest Fruit Decay Caused by the Fungal Pathogen *Botrytis cinerea*. *Genes Genomes Genetics*, 1–18.

Price, J. (2024). *rnaseq_starter*. GitHu*B.* https://githu*B.*com/rj-price/rnaseq_starter

Prins, R. C., & Billerbeck, S. (2024). The signal peptide of yeast killer toxin K2 confers producer self-protection and allows conversion into a modular toxin-immunity system. *Cell Reports*, *43*(7), 114449. https://doi.org/10.1016/j.celrep.2024.114449

R Core Team. (2020). *R: A language and environment for statistical computing. R Foundation for Statistical Computing, Vienna, Austria.* https://www.r-project.org/.

Raivo, H. (2018). *pheatmap: Pretty Heatmaps*. Version 1.0.12. R Package. https://cran.r-project.org/package=pheatmap

Reese, A. J., & Doering, T. L. (2003). Cell wall α-1,3-glucan is required to anchor the Cryptococcus neoformans capsule. *Molecular Microbiology*, *50*(4), 1401–1409. https://doi.org/10.1046/j.1365-2958.2003.03780.x

Reyes-Bravo, P., Acuña-Fontecilla, A., Rosales, I. M., & Godoy, L. (2022). Non-conventional yeasts as biocontrol agents against fungal pathogens related to postharvest diseases. *Sydowia*, *74*(August), 71–78. https://doi.org/10.12905/0380.sydowia74-2021-0071

Ries, S. M. (1995). *RPD No. 704 - Gray Mold of Strawberry*. https://ipm.illinois.edu/diseases/series700/rpd704/

Ritz, C., & Streibig, J. C. (2005). Bioassay analysis using R. *Journal of Statistical Software*, *12*(5), 1–22. https://doi.org/10.18637/jss.v012.i05

Safitri, D., Wiyono, S., Soekarno, *B.* P. W., & Achmad. (2021). Epiphytic yeasts from piperaceae as biocontrol agents for foot rot of black pepper caused by Phytophthora capsici. *Biodiversitas*, *22*(4), 1895–1901. https://doi.org/10.13057/biodiv/d220436

Sewelam, N., El-Shetehy, M., Mauch, *F.*, & Maurino, V. (2021). Combined Abiotic Stresses Repress Defense and Cell Wall. *Plants*, *10*(1946).

Simão, *F.* A., Waterhouse, R. M., Ioannidis, P., Kriventseva, E. V, & Zdobnov, E. M. (2015). Genome analysis BUSCO : assessing genome assembly and annotation completeness with single-copy orthologs. *Bioinformatics*, *31*(19), 3210–3212. https://doi.org/10.1093/bioinformatics/btv351

Smit, A., Hubley, R., & Green, P. (n.d.). *RepeatMasker Open-4.0.* https://www.repeatmasker.org/

Souibgui, E., Bruel, C., Choquer, M., de Vallée, A., Dieryckx, C., Dupuy, J. W., Latorse, M. P., Rascle, C., & Poussereau, N. (2021). Clathrin Is Important for Virulence Factors Delivery in the Necrotrophic Fungus *Botrytis cinerea*. *Frontiers in Plant Science*, *12*(June), 1–15. https://doi.org/10.3389/fpls.2021.668937

Sperschneider, J., & Dodds, P. N. (2022). EffectorP 3.0: Prediction of Apoplastic and Cytoplasmic Effectors in Fungi and Oomycetes. *Molecular Plant-Microbe Interactions*, *35*(2), 146–156. https://doi.org/10.1094/MPMI-08-21-0201-R

Stanke, M., Diekhans, M., Baertsch, R., & Haussler, D. (2008). Using native and syntenically mapped cDNA alignments to improve de novo gene finding. *Bioinformatics*, *24*(5), 637–644. https://doi.org/10.1093/bioinformatics/btn013

Sutton, J. C. (1990). Epidemiology and management of *Botrytis* leaf blight of onion and gray mold of strawberry : a comparative analysis. *Canadian Journal of Plant Pathoglogy*, *12*(1), 37–41. https://doi.org/10.1080/07060669009501048

Tang, J. (2022). *dishy*. GitHu*B.* https://githu*B.*com/jeremyt0/dishy

Teufel, *F.*, Almagro Armenteros, J. J., Johansen, A. R., Gíslason, M. H., Pihl, S. I., Tsirigos, K. D., Winther, O., Brunak, S., von Heijne, G., & Nielsen, H. (2022). SignalP 6.0 predicts all five types of signal peptides using protein language models. *Nature Biotechnology*, *40*(7), 1023–1025. https://doi.org/10.1038/s41587-021-01156-3

Tierens, K. *F.* M. J., Thomma, *B.* P. H. J., Bari, R. P., Garmier, M., Eggermont, K., Brouwer, M., Penninckx, I. A. M. A., Broekaert, W. *F.*, & Cammue, *B.* P. A. (2002). Esa1, an *Arabidopsis* mutant with enhanced susceptibility to a range of necrotrophic fungal pathogens, shows a distorted induction of defense responses by reactive oxygen generating compounds. *Plant Journal*, *29*(2), 131–140. https://doi.org/10.1046/j.1365-313x.2002.01199.x

Travers-Cook, T. J., Jokela, J., & Buser, C. C. (2023). The evolutionary ecology of fungal killer phenotypes. *Proceedings of the Royal Society B: Biological Sciences*, *290*(2005).

https://doi.org/10.1098/rsp*B.*2023.1108

Trenberth, K. E. (2011). Changes in precipitation with climate change. *Climate Research*, *47*(1–2), 123–138. https://doi.org/10.3354/cr00953

Van der Auwera, G. A., & O'Connor, *B.* D. (2020). *Genomics in the Cloud: Using Docker, GATK, and WDL in Terra* (1st Editio). O'Reilly Media.

Varadi, M., Bertoni, D., Magana, P., Paramval, U., Pidruchna, I., Radhakrishnan, M., Tsenkov, M., Nair, S., Mirdita, M., Yeo, J., Kovalevskiy, O., Tuny, K., Žídek, A., Tomlinson, H., Hariharan, D., Abrahamson, J., Green, T., Jumper, J., Hassabis, D., & Velankar, S. (2024). AlphaFold Protein Structure Database in 2024: providing structure coverage for over 214 million protein sequences. *Nucleic Acids Research*, *52*, D368–D375.

Whyte, J. R. C., & Munro, S. (2001). A yeast homolog of the mammalian mannose 6-phosphate receptors contributes to the sorting of vacuolar hydrolases. *Current Biology*, *11*, 1074–1078.

*World Population Prospects*. (2024). Online Edition.

Zhang, Yanjun, Seeram, N., Lee, R., Feng, L., & Heber, D. (2008). Isolation and Identification of Strawberry Phenolics with Antioxidant and Human Cancer Cell Antiproliferative Properties. *Journal of Agricultural and Food Chemistry*, *56*, 670–675. https://doi.org/10.1021/jf071989c

Zhang, Yi, Zhang, Y., Qiu, D., Zeng, H., Guo, L., & Yang, X. (2015). BcGs1, a glycoprotein from *Botrytis cinerea*, elicits defence response and improves disease resistance in host plants. *Biochemical and Biophysical Research Communications*, *457*(4), 627–634. https://doi.org/10.1016/j.bbrc.2015.01.038